Chapter 7

# Good Practice for Fatigue Crack Growth Curves Description

Sylwester Kłysz and Andrzej Leski

Additional information is available at the end of the chapter

http://dx.doi.org/10.5772/52794

## 1. Introduction

Fatigue life estimation and crack propagation description are the most important components in the analysis of life span of structural components but it may require time and expense to investigate it experimentally. For fatigue crack propagation studying in cases when it is difficult to obtain detailed results by direct experimentation computer simulation is especially useful. Hence, to be efficient, the crack propagation and durability of construction or structural component software should estimate the remaining life both experimentally and by simulation. The critical size of the crack or critical component load can be calculated using material constants which have been derived experimentally and from the constant amplitude crack propagation curve, crack size-life data and curve using crack propagation software. Many works in the field of fracture mechanics prove significant development in the numerical analysis of test data from fatigue crack propagation tests.

A simple stochastic crack growth analysis method is the maximum likelihood and the second moment approximation method, where the crack growth rate is considered as a random variable. A deterministic differential equation is used for the crack growth rate, while it is assumed that parameters in this equation are random variables. The analytical methods are implemented into engineering practice and are use to estimate of the statistics of the crack growth behavior (Elber, 1970; Forman et al., 1967; Smith, 1986).

Though many models have been developed, none of them enjoys universal acceptance. Due to the number and complexity of mechanisms involved in this problem, there are probably as many equations as there are researchers in the field. Each model can only account for one or several phenomenological factors - the applicability of each varies from case to case, there is no general agreement among the researchers to select any fatigue crack growth model in relation to the concept of fatigue crack behavior (Kłysz, 2001; Paris & Erdogan, 1963; Wheeler, 1972; Willenborg et al., 1971). Mathematical models proposed e.g. by Paris,

Forman, and further modifications thereof describe crack propagation with account taken of such factors as: material properties, geometry of a test specimen/structural component, the acting loads and the sequence of these loads (AFGROW, 2002; Kłysz et al., 2010a; NASGRO®, 2006; Newman, (1992); Skorupa, 1996). Application of the NASGRO equation, derived by Forman and Newman from NASA, de Koning from NLR and Henriksen from ESA, of the general form (AFGROW, 2002; NASGRO, 2006):

$$\frac{da}{dN} = C \cdot \left[ \frac{(1-f)}{(1-R)} \cdot \Delta K \right]^n \cdot \frac{\left(1 - \frac{\Delta K_{th}}{\Delta K}\right)^p}{\left(1 - \frac{K_{\max}}{K_c}\right)^q} \tag{1}$$

has significantly extended possibilities of describing the crack growth rate tested according to the standard (ASTM E647). The coefficients stand for:

$a$ – crack length [mm],
$N$ – number of load cycles,
$C$, $n$, $p$, $q$ – empirical coefficients,
$R$ – stress ratio,
$\Delta K$ – the stress-intensity-factor (SIF) range that depends on the size of the specimen, applied loads, crack length, $\Delta K = K_{max} - K_{min}$ $[MPa\sqrt{m}]$,
$\Delta K_{th}$ – the SIF threshold, i.e. minimum value of $\Delta K$, from which the crack starts to propagate:

$$\Delta K_{th} = \left( \Delta K_1 \cdot \left( \frac{a}{a + a_0} \right)^{\frac{1}{2}} \right) \cdot \frac{\left[ \frac{1-R}{1-f} \right]^{(1+R \cdot C_{th})}}{(1-A_0)^{(1-R) \cdot C_{th}}} \tag{2}$$

or

$$\Delta K_{th} = \left( \Delta K_0 \cdot \left( \frac{a}{a + a_0} \right)^{\frac{1}{2}} \right) / \left( \frac{1-f}{(1-A_0)(1-R)} \right)^{(1+C_{th}R)} \tag{2a}$$

where: $a_0$ – structural crack length that depends on the material grain size [mm],

$\Delta K_0$ – threshold SIF at $R \to 0$,
$\Delta K_1$ – threshold SIF at $R \to 1$,
$C_{th}$ – curve control coefficient for different values of $R$; equals 0 for negative $R$, equals 1 for $R \geq 0$, for some materials it can be found in the NASGRO database,
$K_{max}$ – the SIF for maximum loading force in the cycle,
$K_c$ – critical value of SIF,
$f$ – Newman's function that describes the crack closure:

$$f = \begin{cases} \max\left(R, A_0 + A_1 R + A_2 R^2 + A_3 R^3\right) & for \quad R \geq 0 \\ A_0 + A_1 R & for \quad -2 \leq R < 0 \end{cases} \tag{3}$$

where $A_0$, $A_1$, $A_2$, $A_3$ coefficients are equal:

$$A_0 = (0.825 - 0.34 \cdot \alpha + 0.05 \cdot \alpha^2) \cdot \left[\cos\left(\frac{\pi}{2} \cdot \frac{S_{\max}}{\sigma_0}\right)\right]^{\frac{1}{\alpha}}, \tag{4}$$

$$A_1 = (0.415 - 0.071 \cdot \alpha) \cdot \frac{S_{\max}}{\sigma_0}, \tag{5}$$

$$A_2 = 1 - A_0 - A_1 - A_3, \tag{6}$$

$$A_3 = 2 \cdot A_0 + A_1 - 1. \tag{7}$$

$\alpha$, $S_{max}/\sigma_0$ – Newman's empirical coefficients.

Determination of the above coefficients for equation that correctly approximates test data is difficult and causes some singularities described below, when the Least Squares Method (LSM) is used.

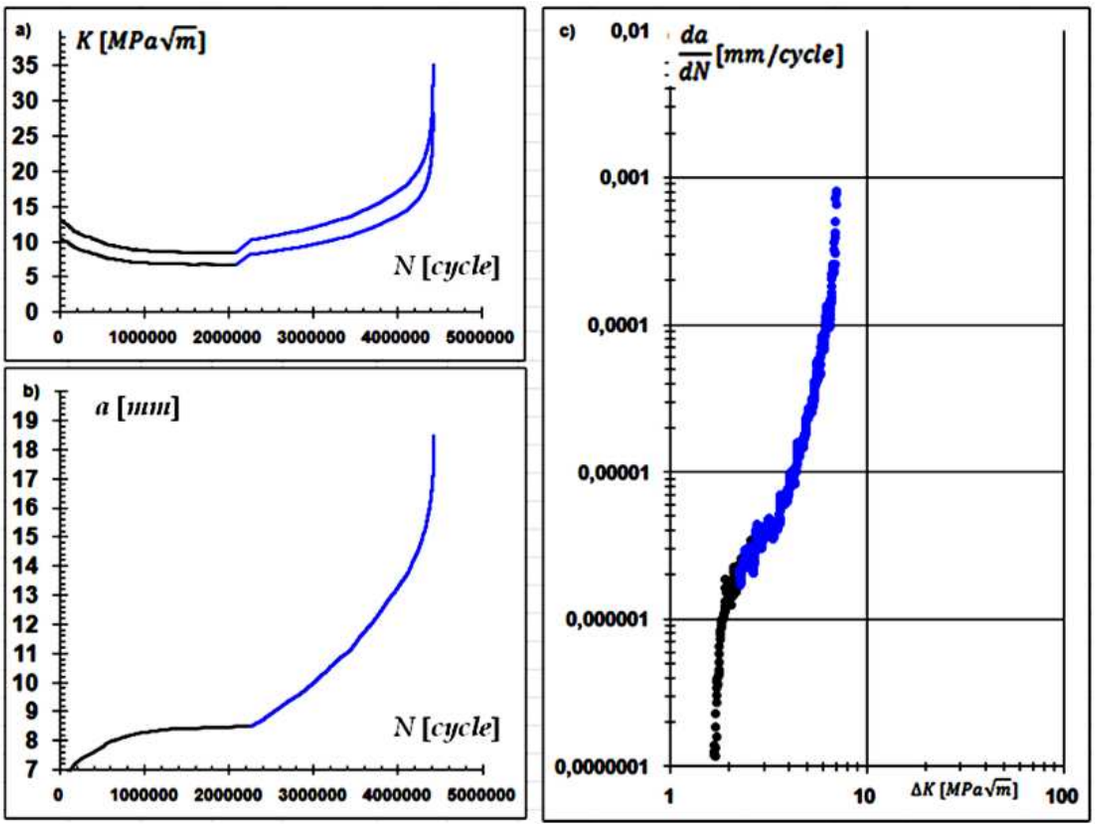


**Figure 1.** Fatigue crack propagation graphs: a) *K=f(N)*; b) *a=f(N)* and c) *da/dN=f(ΔK)*

The fatigue crack growth test results provide an illustration of relations such as: specimen stress intensity vs. number of cycles (*K=f(N)*), crack growth vs. number of cycles (*a=f(N)*); crack growth rate vs. stress intensity factor range (*da/dN=f(ΔK)*). These experimental curves can be presented, for example, in the graphical form shown in Fig. 1 (for a single specimen, two-stage test: stage I - decreasing $\Delta K$ test, black curve; stage II – constant amplitude test, blue curve).

Specifically, the *da/dN=f(ΔK)* plots can be obtained directly from the material test machine control software (e.g. by employing the compliance method and by using a clip gauge) or can be obtained by differentiating the *a=f(N) c*urve after correlating it with *K=f(N)*. These plots, for single specimen tests, as well as for tests with multiple specimens under different load conditions (e.g. various stress ratio *R* values), can be successfully described analytically when appropriate mathematical models and equations are employed.

## 2. Test data

Fatigue tests for structural components durability analysis can be conducted with the RCT (*Round Compact Tension*) (Fig. 2a) or with SEN (*Single Edge Notch*) (Fig. 2b) or other specimens according to the corresponding ASTM E647 standard.

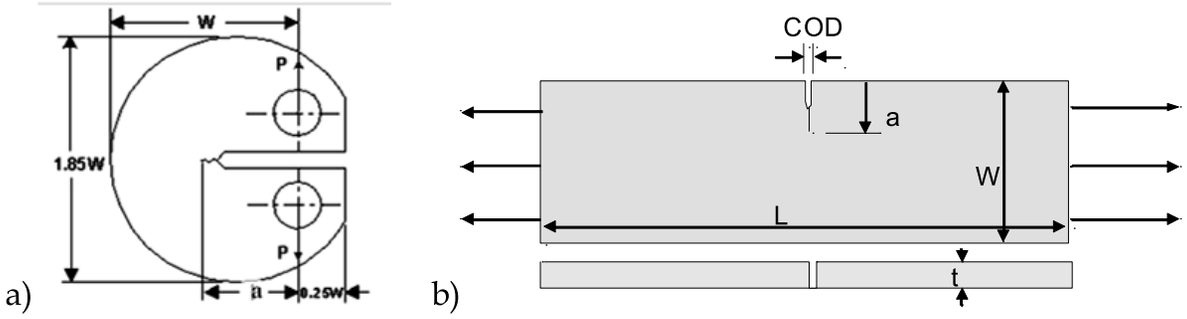


**Figure 2.** RCT & SEN specimens for fatigue crack propagation tests

The general formula that describes the stress intensity factor is as follows:

$$K_I = \frac{P}{B\sqrt{W}} Y, \tag{8}$$

where: $P$ – applied force,
$B$, $W$ – the specimen's thickness and width,
$Y$ – the specimen's shape function (ASTM E647, Fuchs & Stephens 1980, Murakami 1987):
for the RCT specimen:

$$Y = \frac{\left(2+\frac{a}{W}\right)}{\left(1-\frac{a}{W}\right)^{\frac{1}{2}}} \cdot \left(0.886 + 4.64 \cdot \frac{a}{W} - 13.32 \cdot \left(\frac{a}{W}\right)^2 + 14.72 \cdot \left(\frac{a}{W}\right)^3 - 5.56 \cdot \left(\frac{a}{W}\right)^4\right) \tag{9}$$

for the SEN specimen:

$$Y = 1{,}12 - 0{,}231\left(\frac{a}{W}\right) + 10{,}55\left(\frac{a}{W}\right)^2 - 21{,}72\left(\frac{a}{W}\right)^3 + 30{,}39\left(\frac{a}{W}\right)^4 \tag{10}$$

where $a/W$ is a non-dimensional crack length.

The compliance function to compute the crack length in the RCT specimen has the form:

$$\frac{a}{W} = 1 - 4.459\,u + 2.066\,u^2 - 13.041\,u^3 + 167.627\,u^4 - 481.4\,u^5 \tag{11}$$

for the SEN specimen (Bukowski & Kłysz 2003):

$$\frac{a}{W} = 1.407 - 4.132\,u + 3.928\,u^2 - 1.364\,u^3 \tag{12}$$

where: $u$ – compliance described by the following formula:

$$u = \frac{1}{1 + \left(\frac{E \cdot B \cdot COD}{F}\right)^{0.5}}, \tag{13}$$

$E$ – Young's modulus,
$COD$ – Crack Opening Displacement.

An example of the *F-COD* relationship has been plotted in Fig. 3. The plot has been gained from the fatigue crack growth test conducted for the SEN specimen made from constructional steel subjected to constant amplitude loading with overloads (Bukowski & Kłysz, 2003). The records were taken in the course of statically applied 2-cycle overloads of 40% order at subsequent stages of crack propagation. Load base level and overload level were gradually reduced as the crack growth kept increasing and after non-linearity (hysteresis loop) had occurred in the *F-COD* plot. The objective was to avoid failure of the specimen in a subsequent overload cycle to be able then to continue the crack-propagation test. Any change in the angle of inclination of the rectilinear segment of each of the hysteresis loops (i.e. the *F/COD* proportion from formula (13)) is a measure of the specimen's compliance $u$ and proves the crack length in the specimen under examination keeps growing.

Results presented below come from the examination of the 2024 aluminum alloy taken from the helicopter rotor blades (Kłysz & Lisiecki, 2009) or from the aircraft ORLIK's fuselage skins (Kłysz et al., 2010b) and are obtained for three values of test stress ratio $R$ = 0.1; 0.5; 0.8, under laboratory conditions, with loading frequency 15 Hz. The crack length was measured with the *COD clip gauge* using the compliance method. The crack growth rate was determined using the polynomial method.

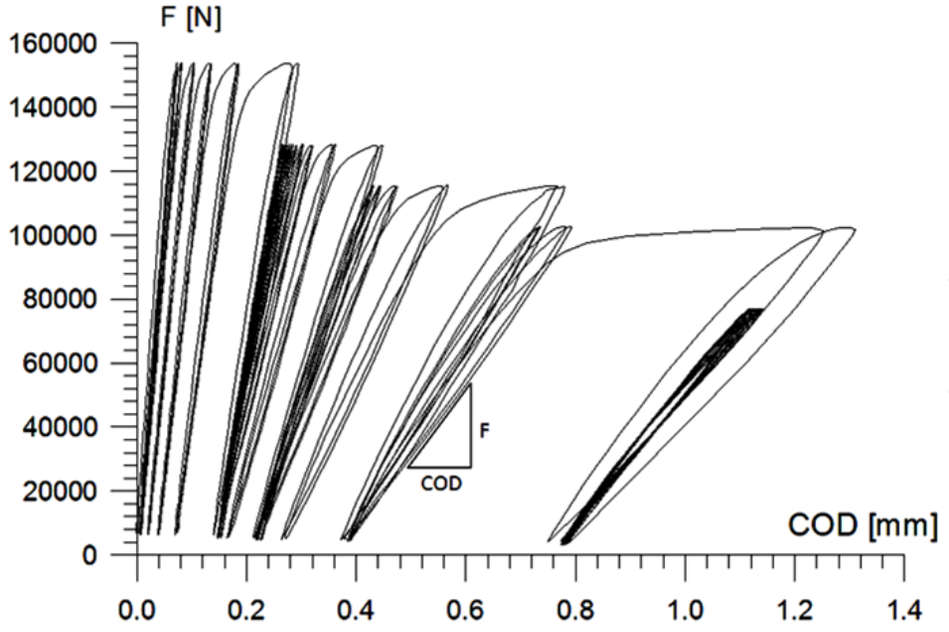


**Figure 3.** Relationship of *F-COD* recorded in subsequent overload cycles of fatigue crack growth test

## 3. Data analysis

Results of fatigue crack growth rate tests for 3 specimens (for $R = 0.1; 0.5; 0.8$) are presented in Fig. 4 (Lisiecki & Kłysz, 2007).

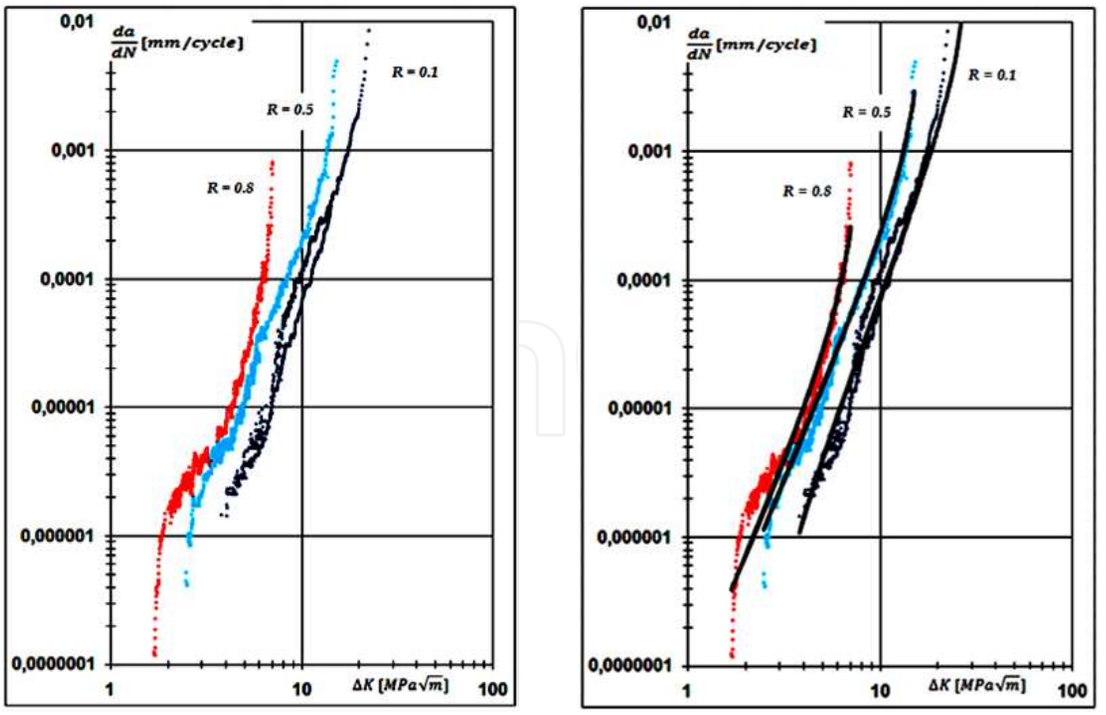


**Figure 4.** Fatigue crack growth rates in 3 specimens for different $R$ values – a) test data, b) results of approximation

The NASMAT curve fitting algorithms use the least-squares error minimization routines in the log-log domain to obtain the corresponding constants using the NASMAT module contained within the NASGRO suite of software (NASGRO, 2006). The constants *C* and *n*, i.e. the main fit parameters, are determined through the minimization of the sum of squares of errors, where the error term corresponding to the *i-th* data pair ($\Delta K$, $da/dN$)$_i$ is (Forman et al., 2005):

$$e_i = \log\left(\frac{da}{dN}\right)_i - \log C - n\log\left[\frac{(1-f)}{(1-R)}\cdot\Delta K\right]_i - \log\cdot\left[\frac{\left(1-\frac{\Delta K_{th}}{\Delta K}\right)^p}{\left(1-\frac{K_{\max}}{K_c}\right)^q}\right]_i. \tag{14}$$

Values of $da/dN$ are determined using the method of differentiating the dependence *a-N* with the secant or the polynomial method applied (AFGROW, 2002; ASTM 647; NASGRO, 2006).

Generally the curve fitting of crack growth data is an iterate process that consists in using established values of various constants (other than *C* and *n*), specifying the data sets that typify the material, applying the least-squares algorithm to compute *C* and *n,* and plotting the data for various *R* values with the curve fit of each stress ratio. The process is continued by making slight modifications in the entered values until the best fit to the test data is obtained. In general fitting the NASGRO equation is really a multi-step process involving:

- fitting or defining the threshold region;
- fitting or defining the critical stress intensity or toughness to be used at the instability asymptote;
- making initial assumptions on key parameters such as *p* and *q*;
- performing the least squares fit to obtain *C* and *n*; and finally;
- using engineering judgment to adjust the results for consistency and/or a desired level of conservatism.

For the LSM approximation of test data, analytical description thereof, and determination of coefficients of approximation equations, according to which the criterion used in the analysis is the minimum of the square sum:

$$S = \sum_{i=1}^{n}\left(\overline{y_i} - y_i\right)^2 \tag{15}$$

of deviations between values of the test data $y_i$ and those of the approximated function $\bar{y}_i$. This method of approximation is characterized with the following properties that in some cases may be considered as disadvantages (Forman et al., 2005; White et al., 2005; Huang et al., 2005; Taheri et al., 2003):

- in respect of the order of magnitude, value of the sum *S* increases as magnitudes of approximated values increase, e.g. if values of test data are of the order of magnitude

10, 1000, 1000000, with the scatter of 10%, the summed differences are of the order of magnitude 1, 100, 100000, and hence, dynamic changes in the total value of the sum *S* depend on values of differences – as a quadratic function it is characterized by a linear function of the derivative, which also means that for differences close to zero (e.g. $10^{-5}$, $10^{-8}$, etc.) this dynamic change is much smaller than for differences of higher magnitudes, which influences the „flexibility" of the performed approximation;

- if the test data significantly differ from each other in magnitude (e.g. from 1 to 100000 or from $10^{-8}$ to $10^{-2}$), the approximated values near the lower threshold contribute much less to the total sum *S* than approximated values near the upper threshold; this means that, e.g. tens or hundreds of test data with differences in magnitude of 100% from value 1 are less significant in performing the approximation than one or a few data points which differ by 1% from value 100000.

According to the above stated example, the approximation is "asymmetric" since better approximation will be achieved for higher values of test data, neglecting differences around smaller values – an example of such approximation is shown in Fig. 4b, where one can see a good fit of theoretical description of 3 curves for large values of *da*/*dN* (over $10^{-4}$ mm/cycle) while there is an evident misfit for smallest values (below $10^{-5}$ mm/cycle). The presented approximation has been achieved by satisfying the LSM criterion, i.e. the minimum value of the sum *S*. When the test data are within a wide range of values, e.g. 5 orders of magnitude, i.e. from $10^{-2}$ to $10^{-7}$ mm/cycle, then differences between the highest values and the approximating function will have the largest effect on the square sum *S* of deviations while differences for small values, sometimes of 2-3 orders of magnitude, do not contribute much to the total sum *S*.

Hence, the misfit of the approximating function for low values of *da*/*dN*, practically for values lower by only 1-2 orders of magnitude than the maximum values of *da*/*dN*. Within this range the theoretical description is rather random and has rather no effect on the value of the sum *S*, which indicates that this criterion is rather useless for this type of analysis.

It seems reasonable to use one of the following criterion modifications, which will allow to remove the above stated problems:

- changing the form of the criterion, or
- using logarithmic values of *da*/*dN*,

$$S = \sum_{i=1}^{n} \left( \overline{\log y_i} - \log y_i \right)^2 \qquad or \qquad S = \sum_{i=1}^{n} \left( \log \overline{y_i} - \log y_i \right)^2 . \tag{16}$$

In the present study the first variant has been examined (see section 3.3) due to the fact that it is more general since it does not limit itself only to positive values of predicted $y_i$, which is a requirement in the second variant. In the case of crack propagation test data all the *da*/*dN* values are positive; therefore the second variant could also be used.

Since the criterion for fitting the theoretical description to the test data in the form of equation (15) or (16), or any other, is closely connected with the number of approximated

points (in the case under discussion, coordinates in the graph ($da/dN_i$,$\Delta K_i$)), the quality of fit has to depend on:

- the distribution of the number of test points among particular curves,
- the distribution of test points on particular curves,

not to mention

- the scatter of test points and accuracy of finding them.

If the distribution of points among particular curves is not uniform, the approximation will show better fit *to the curves* with a larger number of points than to those with a smaller number of points – the contribution thereof to the pooled error included in the approximation criterion will be greater; the minimization thereof will occur around the larger data cluster. Similar situation occurs while fitting the description *to a given* experimentally gained *curve* – where the data concentration is larger, the approximation will be better than where there is less data, or where the data are only individual points. Therefore, essential to the analysis of test data and to description thereof is the regular distribution of the test data over the whole range to be subject to approximation. Since it is sometimes beyond the reach of researchers while recording the test data directly during the testing work, some modification or recalculation of the test data set may prove indispensable.

### 3.1. Data set modification

As clearly seen in Fig. 4, the number of points in the threshold and critical areas of the scope of the stress intensity factor $\Delta K$ is very small, which results from the specific nature of the performed test and data recording.

For crack growth rates lower than $10^{-6}$ mm/cycle the increment by 1 mm occurs after approx. 1 million cycles, i.e. the process is a long-lasting one, and the recording of the crack-length increment for instance every 0.01 mm gives 100 points of test data only (while in the case of taking records every 0.005 mm, the number of points will be 200). The testing work for even lower crack growth rates is still more time- and energy-consuming. With as little crack-length increments as these there is practically no chance that in single load cycles any random jump will occur in values of recorded data of the order of 0.01 or at least 0.001 mm (i.e. by approximately 3 – 4 orders of magnitude higher than the crack growth rate under examination). This provides relatively regular recording of crack lengths in the course of the testing work, i.e. for subsequent increments 0.01, 0.02, 0.03, … mm, etc. (even if measurements are taken for crack-length increments by only a fraction of a millimetre, i.e. in a shorter time, which means for the number of cycles lower than the above-mentioned 1 million).

In the range of critical crack propagation, at the crack growth rate higher than $10^{-3}$ mm/cycle, the recordings of the crack length increments every 0.01 mm (as above) take place more frequently than every 10 cycles. For load-applying frequencies of 10 – 20 Hz this means 1 s

long data-recording intervals in the course of the testing work. The final several millimetres' crack-length increment occurs as fast as over only several minutes of the testing work, with crack-length increments significantly increasing every cycle. Hence, at the testing rate getting as high, the number of test points remains relatively low and, because of these ever-growing increments, lower than the above-mentioned 100 or 200 points per every 1 mm of the crack length.

In the intermediate area of the graph ($10^{-6}$ through $10^{-3}$ mm/cycle, i.e. covering 3 orders of magnitude of the $da/dN$ value) the above-mentioned exemplary crack-length increments every 0.01 mm take place on a regular basis, however, with random fluctuations typical of the phenomenon under examination – there are no identical data recordings after 0.01, 0.02, 0.03, 0.04, … mm of crack-length increment, since instantaneous readings (variations) from the measuring sensors may cause that the data recording during the test, with the same recording criterion assumed, can occur for increments of, e.g. 0.01, 0.028, 0.038, 0.057, … mm, disturbing at the same time the regular basis of increments in the number of cycles between particular measurements. Fig. 5a illustrates the non-uniformity of such data-recording practice; the arrows point to where such disturbances have occurred, and after which the subsequent record is taken after the higher number of cycles. This, in turn, affects the crack growth rate. Calculation of the $da/dN$ derivative based on the in this way recorded data must also be burdened with a random scatter, Fig. 5b, larger than that resulting from the properties of the material under examination.

To eliminate these incidental disturbances, the experimentally recorded time function may become smoothed by means of interpolation of results on the basis of any linear regression function (with either a straight line or a polynomial). Fig. 5c shows an example of such smoothening: presented with a full line is result of the 7-point regression, i.e. after having interpolated each point ($a_i$;$N_i$), with account taken of 6 adjacent points: 3 points in front of and 3 points behind a given point ($a_i$;$N_i$). It is evident that this smoothed curve represents in a reliable (or even better, in a more reliable way) the experimentally recorded dependence between measured quantities. On the other hand, the above-discussed disturbances have been removed from particular measurements.

Calculation of the $da/dN_i$ derivative for any point of the plot ($a_i$;$N_i$) can be carried out on the basis of linear or polynomial regression for e.g. 5, 7, or 9 adjacent points around a given $i$-th point. Fig. 5d shows result of the 5-point linear regression (2 points in front of the ($a_i$;$N_i$) point, the ($a_i$;$N_i$) point, 2 points behind the ($a_i$;$N_i$) point), of calculations of the $da/dN$ derivative against the unsmoothed plot $a$-$N$. What in this case is arrived at from the equation for the line of regression $y_i = m_i x_i + n_i$ (and more exactly, $a_i = m_i N_i + n_i$) is:

$$da / dN_i = \left(y_i\right)' = m_i. \tag{17}$$

In the case of linear regression with polynomials of the 2nd ($y_i = m_i x_i^2 + n_i x_i + l_i$) or 3rd ($y_i = m_i x_i^3 + n_i x_i^2 + l_i x_i + k_i$) order, the crack growth rate is calculated from the formulae, respectively:

$$da / dN_i = \left(y_i\right)' = 2m_i x_i + n_i, \tag{18}$$

$$da / dN_i = \left(y_i\right)' = 3m_i x_i^2 + 2n_i x_i + l_i. \tag{19}$$

What becomes evident is a considerable scatter of calculated values of the crack growth rate *da*/*dN*, and for points indicated with arrows it can be stated that:

- any measurement disturbance results in that the resulting (calculated) value of *da*/*dN* at one or two subsequent points is always lower than that for the point in question,
- the measurement disturbance is not expected to reflect the accelerated crack propagation, even though in the form of a local maximum, which all the more confirms the correctness of treating this disturbance as a random effect,
- where the disturbance occurs in the local-maximum area, it magnifies its value; however, the scale of this increase may prove too large as compared to the actual crack growth rate.

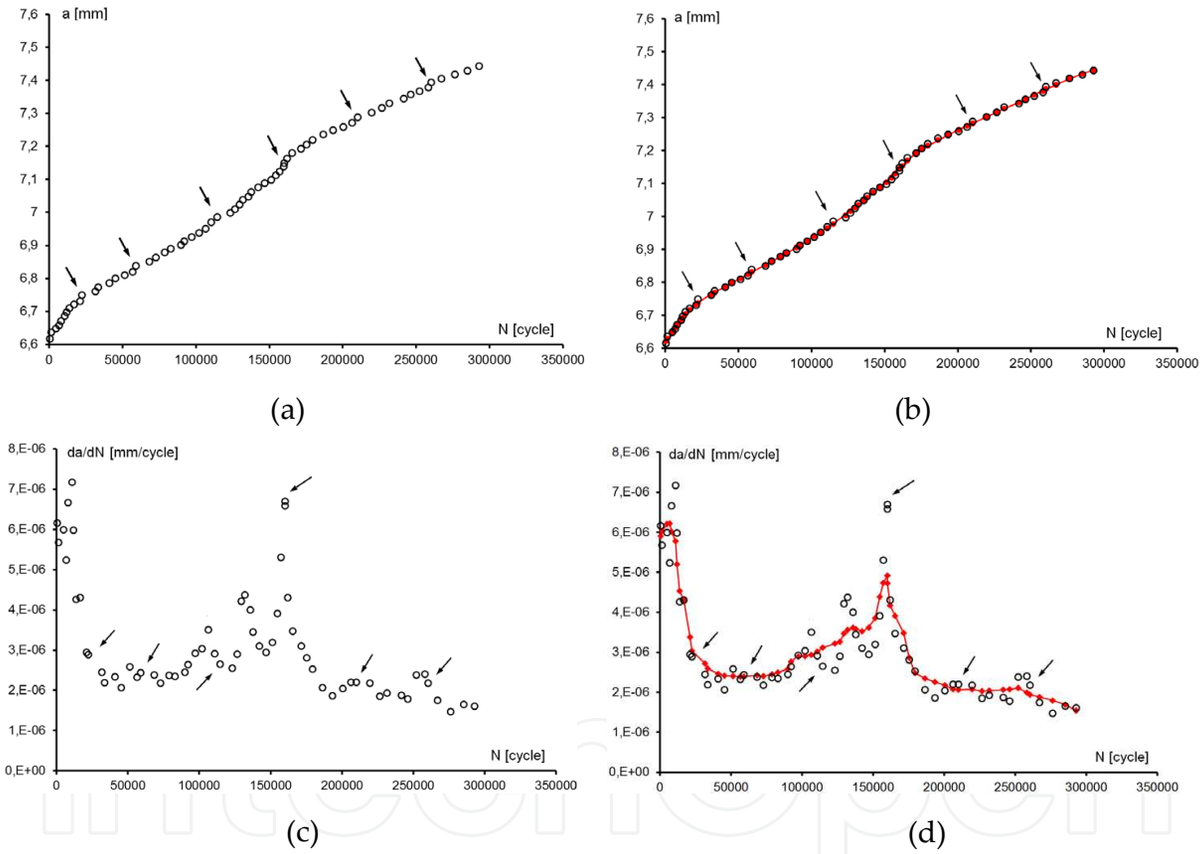


**Figure 5.** Calculated values of *da*/*dN* with corresponding test data *a*-*N*: 5-point linear regression, a) and b) – output data; c) and d) – smoothed data

If calculations are carried out for the smoothed curve *a*-*N* (Fig. 5c), the resulting *da*/*dN* curve presented in Fig. 5d takes the form of a solid line. The scatter of values of the crack growth rate over the whole range of calculations is much smaller. The local extremes have been maintained, however, slightly scaled down than in Fig. 5b.

In the case the regression used to calculate the *da*/*dN* derivative is carried out for a greater number of points adjacent to a given computational point, the corresponding curves look

like in Fig. 5a (for 7-point regressions: 3 points in front of the $(a_i;N_i)$, the point in question $(a_i;N_i)$ and 3 points behind the $(a_i;N_i)$) and Fig. 5b (for 9-point regressions: 4 points in front of the $(a_i;N_i)$, the point in question $(a_i;N_i)$ and 4 behind the $(a_i;N_i)$). In all the cases the derivative of $da/dN$ has been found from equation (17).

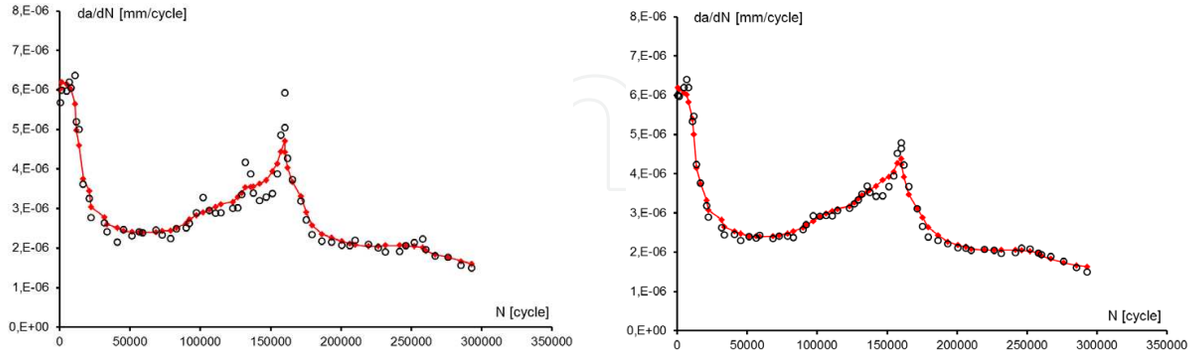


(a) (b)

**Figure 6.** Calculated values of $da/dN$ together with corresponding experimental data $a$-$N$: a) 7-point linear regression, b) 9-point linear regression

It is obvious that as the number of points taken into account in the regression analysis increases, the scatter of computational results gets reduced and the curve plotted for unsmoothed data (circles in Fig. 6) ever more resembles the curve plotted for smoothed data (solid line in Fig. 6). It is effected by the fact that the greater number of data accepted for regression brings the result closer to that of regression for smoothed data. There is of course some disadvantage: the greater number of data taken into account in regression analyses, the more reduced number of details referring to, e.g. local changes in value of $da/dN$ are to be seen on the plotted curves. In the extreme, if all the points are subject to regression at once, the smoothed curve $a$-$N$ would be a straight line and the $da/dN$ curve would run horizontally. Another extreme consists in that the whole curve $a$-$N$ would be described with only one regression equation, which in turn would provide the reliable mapping of the whole $a$-$N$ curve; the $da/dN$ derivative could be calculated by means of differentiating this equation. However feasible, it seems unpractical, work-consuming, more of the 'art for art's sake' category. Results presented in Figs 5 and 6 could be considered optimal: they provide good mapping of local changes in the approximated curves and do not require any complicated mathematical apparatus.

Characteristic of these plots (for both the unsmoothed and smoothed data) is that the calculated rates $da/dN$ may be the same for different numbers of cycles $N$ (hence, for different crack lengths $a$ and different values of $\Delta K$). This is the effect of more common, for this range of crack growth rate $da/dN$, occurrences of changes in the monotonicity of curves $a$-$N$ than in threshold or critical ranges of $da/dN$-$\Delta K$. Curves plotted in Figs 5 and 6 correspond to approx. 1-millimetre increment in the crack length (6.6 through 7.5 mm) and cover crack growth rates of $2 \div 4 \cdot 10^{-6}$ mm/cycle. At the further stage of the crack growth as the crack length increases, the crack growth rate increases as well, and before the crack

reaches the critical growth range the calculated values of *da*/*dN* from the range $10^{-6}$ through $10^{-3}$ mm/cycle will repeatedly appear in the calculations. Hence, the number of measuring points recorded throughout the testing work for this range of *da*/*dN* will be higher than for threshold or critical ranges of *da*/*dN*-Δ*K*, what is to be seen also in Fig. 4.

Moreover, in practice, the plotting of a complete crack propagation curve *da*/*dN*-Δ*K*, i.e. starting from critical crack growth rates of $10^{-8}$ mm/cycle up to critical ones of $10^{-2}$ mm/cycle, is not performed in the course of one test only. This is closely related with difference in levels of Δ*K* for the stage of the specimen's precracking and the threshold range typical of the rates of $10^{-8}$ mm/cycle. The precracking usually finishes at higher values of Δ*K*, since it cannot proceed with the threshold growth rate. The reason is that it would take much more time than the test itself. Therefore, the test started after the specimen's precracking stage from the threshold values of the crack growth (change in the loading level from high to lower), would be connected with the crack growth retardation effect, which - in turn - would disturb test results in this area, i.e. it would not allow the researchers to gain the correct curve *da*/*dN*-Δ*K*. Such tests are usually conducted as a two-stage effort – see Fig. 1:

I stage – with exponentially decreasing Δ*K* ($\Delta K=\Delta K_0 e^{-ga}$), with constant relative gradient, i.e. $\frac{1}{\Delta K}\frac{\partial \Delta K}{\partial a} = -g$, up to having the left side of the plot within the threshold range. The test starts from the level of loads higher than those at the already completed stage of the specimen's precracking, so as to eliminate the crack growth retardation effect that appears as if the test is started at loads lower than those at the termination of the specimen's precracking.

The decreasing Δ*K*, starting from some suitably high value, and the crack length both cause that the crack growth rate becomes reduced to reach then the threshold range of the plot. At this stage, the *a*-*N* curve asymptotically approaches the horizontal line as the testing time increases. The testing time depends on the scientifically and economically justified needs of the researcher, although in practice this time much more depends on sensitivity of applied sensors, since both the level of applied loads and the crack opening size decrease for this range to values comparable to electric noise of the testing machine, which usually results in the test being automatically interrupted and the testing machine being stopped for crack growth rates lower than $10^{-8}$ mm/cycle. The at this stage obtained curve *a*-*N* and the propagation-curve section *da*/*dN*-Δ*K* may look like e.g. those presented in Fig. 7 (to be also seen in Fig. 1b).

II stage – at constant amplitude load (*CA test, constant amplitude test*) up to the acquisition of the right side within the critical range. The test is carried out at the level of loads higher than the level at which the stage I was completed; as the crack length increases, there is a systematic increase in the Δ*K*, up to the moment the critical value is reached, at which the specimen fails. The at this stage obtained curve *a*-*N* and the propagation-curve section *da*/*dN*-Δ*K* may look like e.g. those presented in Fig. 7 (to be also seen in Fig. 4).

The total result of both the stages has been presented in Fig. 8 – both the curves from Figs 6 and 7 complement one another to full propagation-curve plot *a*-*N* and *da*/*dN*-Δ*K*: experimentally found points in the form of circles, curves smoothed in the form of full lines.

It is quite clear that the mid section (range) of the *da*/*dN*-Δ*K* curve contains much more experimentally gained points despite the same criterion for data recording in the course of testing work for all three ranges, and also, independently of the fact that both the curves overlap over some specific section common to both of them. Furthermore, the plot presents the above-discussed changes in the monotonicity of how they run, independently of whether the calculations of the *da*/*dN* derivative have been conducted for unsmoothed or smoothed data – Fig. 8.

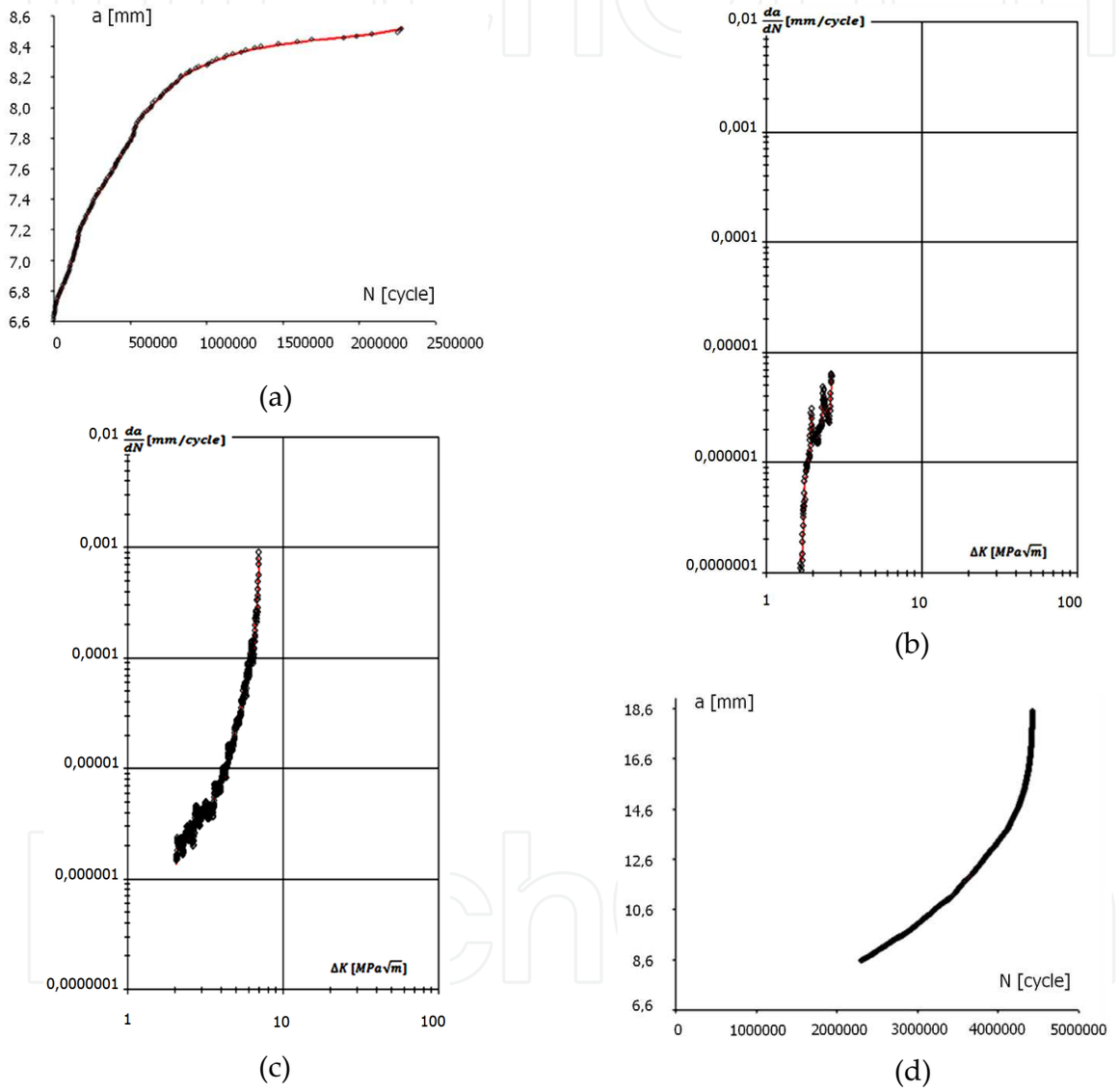


**Figure 7.** Curves *a*-*N* and *da*/*dN*-Δ*K* for the first (I) – a), b), and the second (II) test stages – c), d)

## 3.2. A Method of Regular Curves Mapping (MRCM)

Disturbances in the run, monotonicity of curves *da*/*dN*-Δ*K* as well as different measuring-data density in particular areas of the graph do not serve well any attempts to theoretically describe these curves. As mentioned earlier, the least squares methods better fit regression curves to

areas where there is more approximated points, in the case given consideration, in the middle ranges of the *da/dN*-Δ*K* curves. To eliminate this effect, application of the Authors' Method of Regular Curves Mapping (MRCM) to approximate the *da/dN*-Δ*K* curves is advisable.

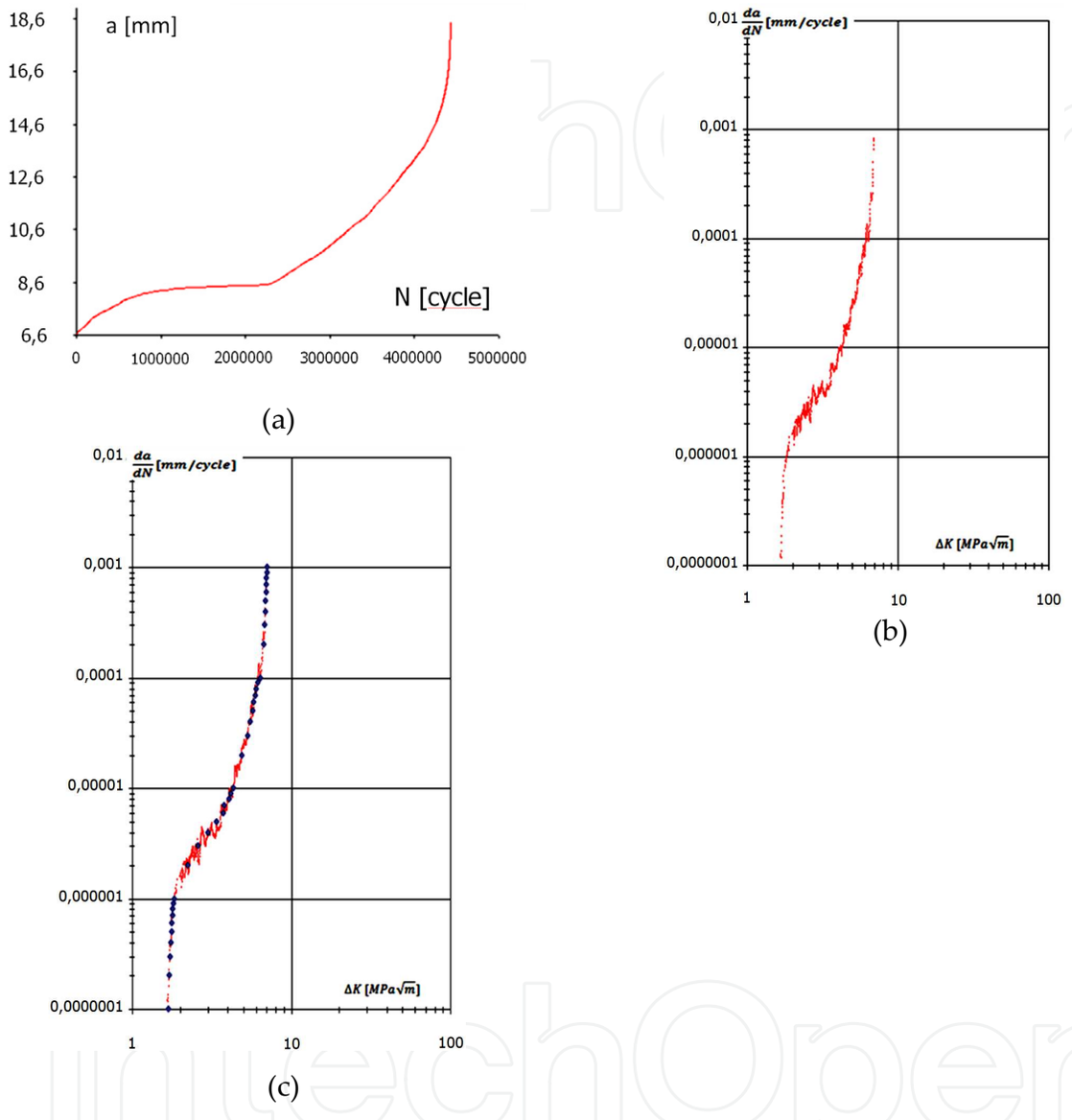


**Figure 8.** Curves *a-N* and *da/dN*-Δ*K* and how they run at the I and II test stages: – results for data after the curve has been smoothed - a), b), and effect of having applied the MRCM – c)

The MRCM technique of mapping test data consists in fixing, at regular intervals (along axes x or y), the *k* number of representative points in the data set under analysis (upon the experimentally gained curve). The following actions are to be taken:

a. determined are selected values of coordinates $x_i$ (or $y_i$), for which the above-mentioned points will be fixed ($i = 1,2, \ldots,k$),
b. from the curve under analysis, point $x'_i$ (or $y'_i$) is fixed, of coordinate value closest to the assumed value of $x_i$ (or $y_i$), and $2m$ of adjacent points – by assumption, in half these are

points of values lower than $x_i$ (or $y_i$) and in half - of higher values, ($m$ is equal to, e.g. 2, 3, 4 or 5),

c. a set of in this way gained data $2m+1$, ($x'_{i-m}$ , $y_{i-m}$) through ($x'_{i+m}$ , $y_{i+m}$) (or ($x_{i-m}$ , $y'_{i-m}$) through ($x_{i+m}$ , $y'_{i+m}$)) – grouped around some selected value of $x_i$ (or $y_i$) is subject to regression with any function to determine the approximated value of $y_i^*$ (or $x_i^*$) corresponding to the selected value of $x_i$ (or $y_i$),

d. the point of coordinates ($x_i$ , $y_i^*$) (or ($x_i^*$, $y_i$)) is mapped on the curve under analysis – as the $i$-th representative data item found on the basis of the assumed criteria,

e. steps b) through d) are repeated for subsequent $k$ number of values determined in a), until a set of $k$ number of points that represent (map) the curve is obtained.

The effect of the in this way performed mapping of values of $da/dN$, regularly distributed within particular intervals (orders of magnitude), in selected $k = 37$ points, for the curve shown in Fig. 8b, is presented in Fig. 8c. The points in question:

- well represent (map) the curve under analysis,
- are equidense distributed within the whole range of $da/dN$ variability,
- do not show any more or less significant fluctuations/scatter of values resulting from, e.g. random measuring-data dispersions.

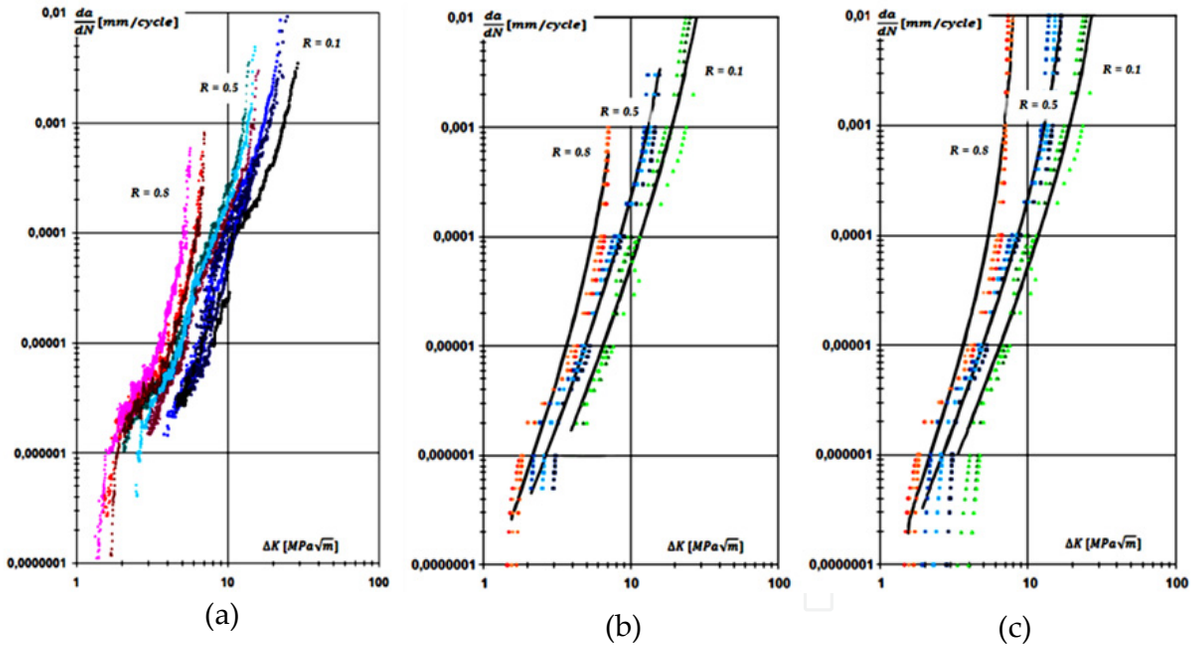


**Figure 9.** Experimentally gained curves $da/dN$-$\Delta K$ for 9 specimens tested at different stress ratios $R$ a) and the same curves having been mapped with points using the MRCM, b) and with extrapolated points that 'perform' the mapping according to the MRCM, c) – together with approximation thereof with the NASGRO equation

The set of points that map the curve seems to give good basis, owing to the above described features, for analyses of theoretical description of a given, experimentally gained curve. In the case of nine (9) curves that correspond to tests with three (3) values of the stress ratio $R$ –

Fig. 9a, the result of experimentally gained data modification with the MRCM applied (points in the graph) is presented in Fig. 9b, together with the data approximation by means of the NASGRO equation, with the LSM criterion used, according to formula (15).

The MRCM technique also enables, if need be and with scientific correctness maintained, the extrapolation of the mapping points *beyond the range* of recorded test data, i.e. into the area of crack growth rates lower (the threshold range) or higher (the critical range) than those recorded experimentally, with their tendency to change which is peculiar to those areas, on the basis of regression at boundary (in the graph – lower or upper) points of experimentally gained curves – the extrapolation result has been shown in Fig. 9c. Application of extrapolation to prepare data for the analytical modelling may prove advantageous in the case the particular experimentally gained curves show different ranges of values, and hence, different numbers of mapping points. After correctly performed extrapolation one can arrive at the situation when they are equalized, which means the same 'power' of each of the with the regression method approximated curves.

### 3.3. Modifications of the LSM method criterion

In order to eliminate the approximation misfit as shown in Fig. 1 and to improve the quality of approximation, modification of formula (15) takes the following form:

$$S^* = \sum_{i=1}^{n} \left( \frac{\overline{y_i} - y_i}{y_i} \right)^2 = \sum_{i=1}^{n} \left( \frac{\overline{y_i}}{y_i} - 1 \right)^2 . \tag{20}$$

The fraction in brackets in formula (13), as a relative error, is a measure of deviation independent of the order of magnitude of compared values (approximated and approximating ones), so that the contribution of all the test data is equally "strong" to the total error $S$, which should have good effect on the approximation within the whole range, since:

- each value among test data $y_i$ has equal contribution to the sum $S^*$, independent of its magnitude $10^{-7}$, $10^{-2}$, 1 or 100000 (i.e. it fits in any magnitude range) – always a deviation of e.g. 10-, 50-, 200-percent of approximating value will give a component of the sum $S^*$ equal to 0.01, 0.25, 4, respectively;
- the criterion assures that the achieved approximation is "symmetric", i.e. the degree of approximation around lower and higher values is the same;
- disadvantages of the criterion described with formula (15) are no longer valid.

The criterion described with formula (20) has also some specific property: if the approximating value equals zero (i.e. for the approximation smaller by 100%) or it is twice as big as the approximated value (i.e. for approximation larger by 100%), then independently of the approximated value the component of the sum $S^*$ will equal 1.

In order to carry out the approximation of test data it is necessary to calculate coefficients of the approximating equation used to determine $\bar{y}_i$. Equation (1), after applying logarithms, takes the form:

$$\log\left(\frac{da}{dN}\right)=\log(C)+n\cdot\log\left[\frac{(1-f)}{(1-R)}\cdot\Delta K\right]+p\cdot\log\left(1-\frac{\Delta K_{th}}{\Delta K}\right)-q\cdot\log\left(1-\frac{K_{\max}}{K_c}\right), \tag{21}$$

and can be presented in the following general way:

$$\bar{y}=b_0+b_1\cdot f_1+b_2\cdot f_2+b_3\cdot f_3. \tag{22}$$

Coefficients $b_i$ are directly connected with $C$, $n$, $p$ and $q$ ($b_0=log(C)$, $b_1=n$, $b_2=p$, $b_3=-q$), whereas functions $f_i$ depend on $\Delta K$ and $R$ and include all the remaining coefficients of the NASGRO equation. Coefficients $b_i$ of the approximating equation are calculated from the minimum condition of the equation (20), i.e.:

$$\frac{\partial S}{\partial b_k}=\frac{\partial\left(\sum_{i=1}^{n}\left(\frac{b_0+b_1\cdot f_{1,i}+b_2\cdot f_{2,i}+b_3\cdot f_{3,i}-y_i}{y_i}\right)^2\right)}{\partial b_k}=0$$
$$k=1,2,3,4. \tag{23}$$

This leads to the following system of equations:

$$\begin{aligned}
\frac{\partial S}{\partial b_0}&=2\cdot\sum_{i=1}^{n}\left[\left(\frac{b_0+b_1\cdot f_{1,i}+b_2\cdot f_{2,i}+b_3\cdot f_{3,i}-y_i}{y_i}\right)\cdot\frac{1}{y_i}\right]=0,\\
\frac{\partial S}{\partial b_1}&=2\cdot\sum_{i=1}^{n}\left[\left(\frac{b_0+b_1\cdot f_{1,i}+b_2\cdot f_{2,i}+b_3\cdot f_{3,i}-y_i}{y_i}\right)\cdot\frac{f_1}{y_i}\right]=0,\\
\frac{\partial S}{\partial b_2}&=2\cdot\sum_{i=1}^{n}\left[\left(\frac{b_0+b_1\cdot f_{1,i}+b_2\cdot f_{2,i}+b_3\cdot f_{3,i}-y_i}{y_i}\right)\cdot\frac{f_2}{y_i}\right]=0,\\
\frac{\partial S}{\partial b_3}&=2\cdot\sum_{i=1}^{n}\left[\left(\frac{b_0+b_1\cdot f_{1,i}+b_2\cdot f_{2,i}+b_3\cdot f_{3,i}-y_i}{y_i}\right)\cdot\frac{f_3}{y_i}\right]=0.
\end{aligned} \tag{24}$$

It is a system of 4 linear equations with 4 unknowns $b_i$, which after transformation takes a form:

$$\begin{aligned}
&n\sum_{i=1}^{n}\frac{1}{y_i}-b_0\sum_{i=1}^{n}\frac{1}{y_i^2}-b_1\sum_{i=1}^{n}\frac{f_{1,i}}{y_i^2}-b_2\sum_{i=1}^{n}\frac{f_{2,i}}{y_i^2}-b_3\sum_{i=1}^{n}\frac{f_{3,i}}{y_i^2}=0,\\
&n\sum_{i=1}^{n}\frac{f_{1,i}}{y_i}-b_0\sum_{i=1}^{n}\frac{f_{1,i}}{y_i^2}-b_1\sum_{i=1}^{n}\frac{f_{1,i}^2}{y_i^2}-b_2\sum_{i=1}^{n}\frac{f_{1,i}f_{2,i}}{y_i^2}-b_3\sum_{i=1}^{n}\frac{f_{1,i}f_{3,i}}{y_i^2}=0,\\
&n\sum_{i=1}^{n}\frac{f_{2,i}}{y_i}-b_0\sum_{i=1}^{n}\frac{f_{2,i}}{y_i^2}-b_1\sum_{i=1}^{n}\frac{f_{1,i}f_{2,i}}{y_i^2}-b_2\sum_{i=1}^{n}\frac{f_{2,i}^2}{y_i^2}-b_3\sum_{i=1}^{n}\frac{f_{2,i}f_{3,i}}{y_i^2}=0,\\
&n\sum_{i=1}^{n}\frac{f_{3,i}}{y_i}-b_0\sum_{i=1}^{n}\frac{f_{3,i}}{y_i^2}-b_1\sum_{i=1}^{n}\frac{f_{1,i}f_{3,i}}{y_i^2}-b_2\sum_{i=1}^{n}\frac{f_{2,i}f_{3,i}}{y_i^2}-b_3\sum_{i=1}^{n}\frac{f_{3,i}^2}{y_i^2}=0.
\end{aligned} \tag{25}$$

and is easily solved by subtracting in the following steps:

- eliminating $b_0$

$$\begin{aligned}
&\frac{n\sum_{i=1}^{n}\frac{1}{y_i}}{\sum_{i=1}^{n}\frac{1}{y_i^2}}-\frac{n\sum_{i=1}^{n}\frac{f_{1,i}}{y_i^2}}{\sum_{i=1}^{n}\frac{f_{1,i}}{y_i^2}}-b_1\left(\frac{\sum_{i=1}^{n}\frac{f_{1,i}}{y_i^2}}{\sum_{i=1}^{n}\frac{1}{y_i^2}}-\frac{\sum_{i=1}^{n}\frac{f_{1,i}^2}{y_i^2}}{\sum_{i=1}^{n}\frac{f_{1,i}}{y_i^2}}\right)-b_2\left(\frac{\sum_{i=1}^{n}\frac{f_{2,i}}{y_i^2}}{\sum_{i=1}^{n}\frac{1}{y_i^2}}-\frac{\sum_{i=1}^{n}\frac{f_{1,i}f_{2,i}}{y_i^2}}{\sum_{i=1}^{n}\frac{f_{1,i}}{y_i^2}}\right)-\\
&-b_3\left(\frac{\sum_{i=1}^{n}\frac{f_{3,i}}{y_i^2}}{\sum_{i=1}^{n}\frac{1}{y_i^2}}-\frac{\sum_{i=1}^{n}\frac{f_{1,i}f_{3,i}}{y_i^2}}{\sum_{i=1}^{n}\frac{f_{1,i}}{y_i^2}}\right)=0,\\
&\frac{n\sum_{i=1}^{n}\frac{1}{y_i}}{\sum_{i=1}^{n}\frac{1}{y_i^2}}-\frac{n\sum_{i=1}^{n}\frac{f_{2,i}}{y_i^2}}{\sum_{i=1}^{n}\frac{f_{2,i}}{y_i^2}}-b_1\left(\frac{\sum_{i=1}^{n}\frac{f_{1,i}}{y_i^2}}{\sum_{i=1}^{n}\frac{1}{y_i^2}}-\frac{\sum_{i=1}^{n}\frac{f_{1,i}f_{2,i}}{y_i^2}}{\sum_{i=1}^{n}\frac{f_{2,i}}{y_i^2}}\right)-b_2\left(\frac{\sum_{i=1}^{n}\frac{f_{2,i}}{y_i^2}}{\sum_{i=1}^{n}\frac{1}{y_i^2}}-\frac{\sum_{i=1}^{n}\frac{f_{2,i}^2}{y_i^2}}{\sum_{i=1}^{n}\frac{f_{2,i}}{y_i^2}}\right)-\\
&-b_3\left(\frac{\sum_{i=1}^{n}\frac{f_{3,i}}{y_i^2}}{\sum_{i=1}^{n}\frac{1}{y_i^2}}-\frac{\sum_{i=1}^{n}\frac{f_{2,i}f_{3,i}}{y_i^2}}{\sum_{i=1}^{n}\frac{f_{2,i}}{y_i^2}}\right)=0,\\
&\frac{n\sum_{i=1}^{n}\frac{1}{y_i}}{\sum_{i=1}^{n}\frac{1}{y_i^2}}-\frac{n\sum_{i=1}^{n}\frac{f_{3,i}}{y_i^2}}{\sum_{i=1}^{n}\frac{f_{3,i}}{y_i^2}}-b_1\left(\frac{\sum_{i=1}^{n}\frac{f_{1,i}}{y_i^2}}{\sum_{i=1}^{n}\frac{1}{y_i^2}}-\frac{\sum_{i=1}^{n}\frac{f_{1,i}f_{3,i}}{y_i^2}}{\sum_{i=1}^{n}\frac{f_{3,i}}{y_i^2}}\right)-b_2\left(\frac{\sum_{i=1}^{n}\frac{f_{2,i}}{y_i^2}}{\sum_{i=1}^{n}\frac{1}{y_i^2}}-\frac{\sum_{i=1}^{n}\frac{f_{2,i}f_{3,i}}{y_i^2}}{\sum_{i=1}^{n}\frac{f_{3,i}}{y_i^2}}\right)-\\
&-b_3\left(\frac{\sum_{i=1}^{n}\frac{f_{3,i}}{y_i^2}}{\sum_{i=1}^{n}\frac{1}{y_i^2}}-\frac{\sum_{i=1}^{n}\frac{f_{3,i}^2}{y_i^2}}{\sum_{i=1}^{n}\frac{f_{3,i}}{y_i^2}}\right)=0
\end{aligned} \tag{26}$$

what gives 3 equations of the general form:

$$\begin{aligned}
&B_k-b_1B_{1,k}-b_2B_{2,k}-b_3B_{3,k}=0\\
&k=\ 1,2,3.
\end{aligned} \tag{27}$$

- eliminating $b_1$

$$\begin{aligned}\frac{B_1}{B_{1,1}}-\frac{B_2}{B_{2,1}}-b_2\left(\frac{B_{1,2}}{B_{1,1}}-\frac{B_{2,2}}{B_{2,1}}\right)-b_3\left(\frac{B_{1,3}}{B_{1,1}}-\frac{B_{2,3}}{B_{2,1}}\right)=0,\\ \frac{B_1}{B_{1,1}}-\frac{B_3}{B_{3,1}}-b_2\left(\frac{B_{1,2}}{B_{1,1}}-\frac{B_{3,2}}{B_{3,1}}\right)-b_3\left(\frac{B_{1,3}}{B_{1,1}}-\frac{B_{3,3}}{B_{3,1}}\right)=0.\end{aligned} \tag{28}$$

what gives 2 equations of the general form:

$$\begin{aligned}&C_k-b_2C_{2,k}-b_3C_{3,k}=0\\ &k=2,3.\end{aligned} \tag{29}$$

- eliminating $b_2$

$$\frac{C_2}{C_{2,2}}-\frac{C_3}{C_{2,3}}-b_3\left(\frac{C_{3,2}}{C_{2,2}}-\frac{C_{3,3}}{C_{2,3}}\right)=0, \tag{30}$$

hence:

$$b_3=\frac{\frac{C_2}{C_{2,2}}-\frac{C_3}{C_{2,3}}}{\frac{C_{3,2}}{C_{2,2}}-\frac{C_{3,3}}{C_{2,3}}}=\frac{\left(\frac{B_1}{B_{1,1}}-\frac{B_2}{B_{2,1}}\right)-\left(\frac{B_1}{B_{1,1}}-\frac{B_3}{B_{3,1}}\right)}{\left(\frac{B_{1,2}}{B_{1,1}}-\frac{B_{2,2}}{B_{2,1}}\right)-\left(\frac{B_{1,2}}{B_{1,1}}-\frac{B_{3,2}}{B_{3,1}}\right)}\cdot\frac{\left(\frac{B_{1,3}}{B_{1,1}}-\frac{B_{2,3}}{B_{2,1}}\right)-\left(\frac{B_{1,3}}{B_{1,1}}-\frac{B_{3,3}}{B_{3,1}}\right)}{\left(\frac{B_{1,2}}{B_{1,1}}-\frac{B_{2,2}}{B_{2,1}}\right)-\left(\frac{B_{1,2}}{B_{1,1}}-\frac{B_{3,2}}{B_{3,1}}\right)}. \tag{31}$$

Hence, coefficient $b_2$ can be calculated from one of the formulae (29); secondly, coefficient $b_1$ from one of equations (27), and finally, coefficient $b_0$ from one of equations (25).

The in this way found coefficients of the NASGRO equation enable approximation of curves $da/dN$-$\Delta K$ from Fig. 9 to the form shown in Fig. 10a. Considerable improvement in the theoretical (analytical) description for the whole range of plotted curves is evident.

Both criteria (15) and (20) have also some disadvantage consisting in that if the approximating value $\bar{y}_i$ is much smaller than the approximated value $y_i$ (i.e. by 3, 5, 7 orders of magnitude) or simply close to zero then the component of the sum $S$ and $S^*$ is close to the squared value $y_i$ (in case of (15)) or to 1 (in case of (20)), independently of how these two values differ from each other.

Obviously, it is important whether the approximation and behavior of the approximating curve near value $y_i$ at the level of e.g. $10^{-6}$ and lower (i.e. for strongly decreasing values within the "threshold" range of the graph) take place at the level of $10^{-8}$, $10^{-12}$ or $10^{-20}$ (what is not hard to achieve for curves showing strong vertical courses on graphs plotted with the

logarithmic scale applied); it is much better when the possible difference between values $\bar{y}_i$ and $y_i$ is not too large.

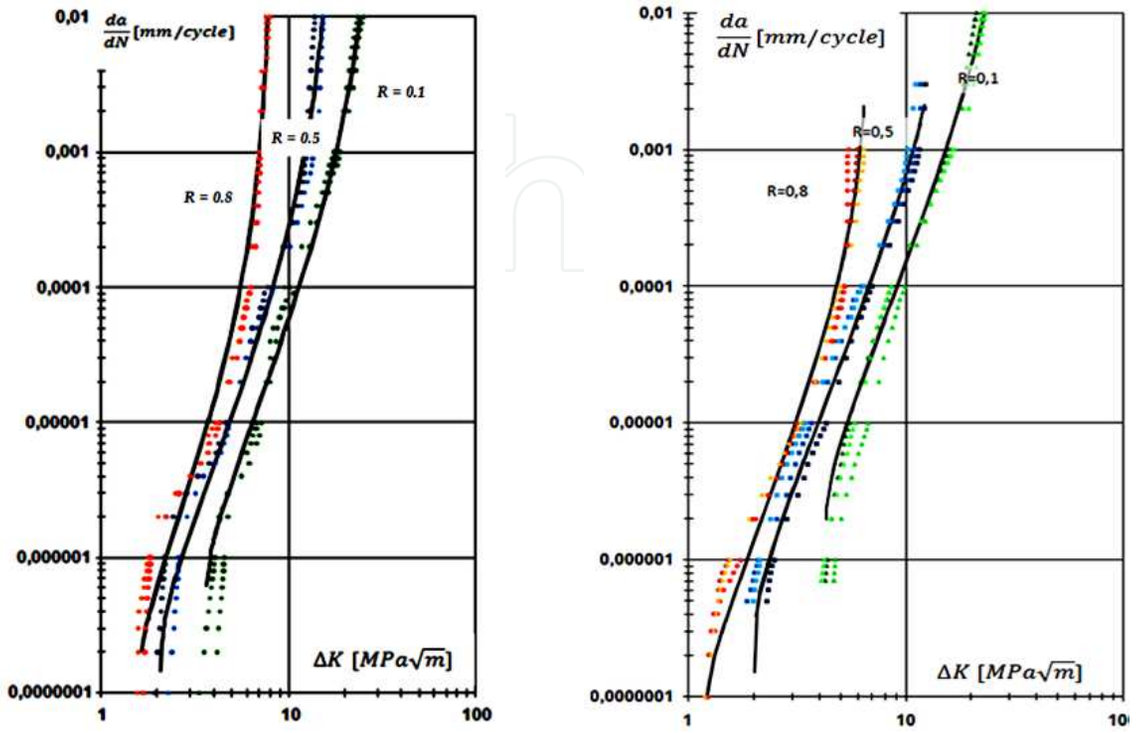


**Figure 10.** Result of approximation of curves from Fig. 9 with the NASGRO equation with the LSM criterion applied: a) by equation (20), b) by equation (32)

Due to dynamic changes around value $\bar{y}_i$ equal to zero (completely monotonic, as for the second-degree polynomial), functions (15) and (20) are practically insensitive to that the approximated value equals e.g. 0.01, $10^{-5}$, $10^{-8}$ or $10^{-20}$. Hence, it is most preferable if the LSM approximating criterion takes such cases into account.

Therefore, a modification is proposed to transform the criterion into the following form:

$$S^{**} = \sum_{i=1}^{n} \left( \frac{\overline{y_i}}{y_i} - 1 \right) \left( 1 - \frac{y_i}{\overline{y_i}} \right). \tag{32}$$

Owing to this for both large values $\bar{y}_i$ (much different from the approximated value $y_i$) and small values (approaching zero) with respect to value $y_i$, the components of the sum take significant values, i.e. in both cases they give a significant (although - as it can be seen - diverse/unsymmetrical for each of the cases) contribution to the total approximation error – as shown in Fig. 11. In order to make the $S_i$ components of the sum (32) and the total sum $S^{**}$ as an approximation criterion reaches the minimum (not the maximum, as in Fig. 11) and also, when the reversal of sign takes place between the approximated value $y_i$ and the approximating value $\bar{y}_i$), the following form would be better:

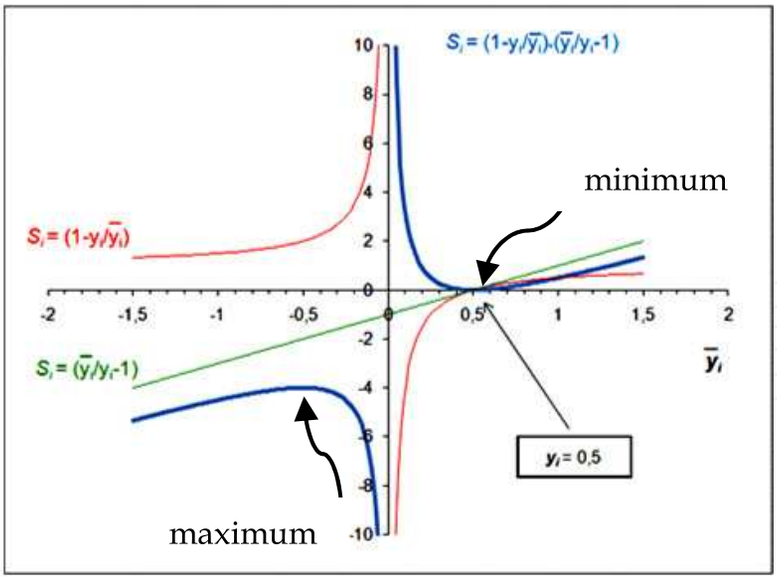


**Figure 11.** Component of the sum for the approximation criterion (32)

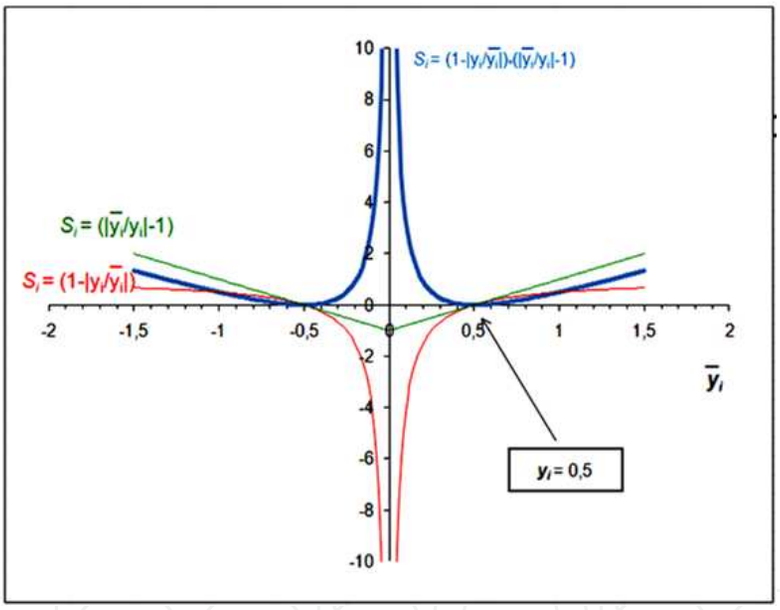


**Figure 12.** Component of the sum for the approximation criterion (32a)

$$S^{**} = \sum_{i=1}^{n}\left(\left|\frac{\bar{y}_i}{y_i}\right| - 1\right)\left(1 - \left|\frac{y_i}{\bar{y}_i}\right|\right). \tag{32a}$$

Both extremes of the $S_i$ function for both positive and negative values of $\bar{y}_i$ are the minima shown in Fig. 12. Approximation criterion functions for (15), (20) and (32) (and their components) as related to approximating values $\bar{y}_i$, for:

- different approximated values $y_i$ equal to 5; 2; 1; 0.25; 0.01; 0.00001,
- the same range of variability of $\bar{y}_i$, i.e. ($-3y_i$, $3y_i$), in order to show the $\bar{y}_i \to 0$ effect, are shown in Fig. 13.

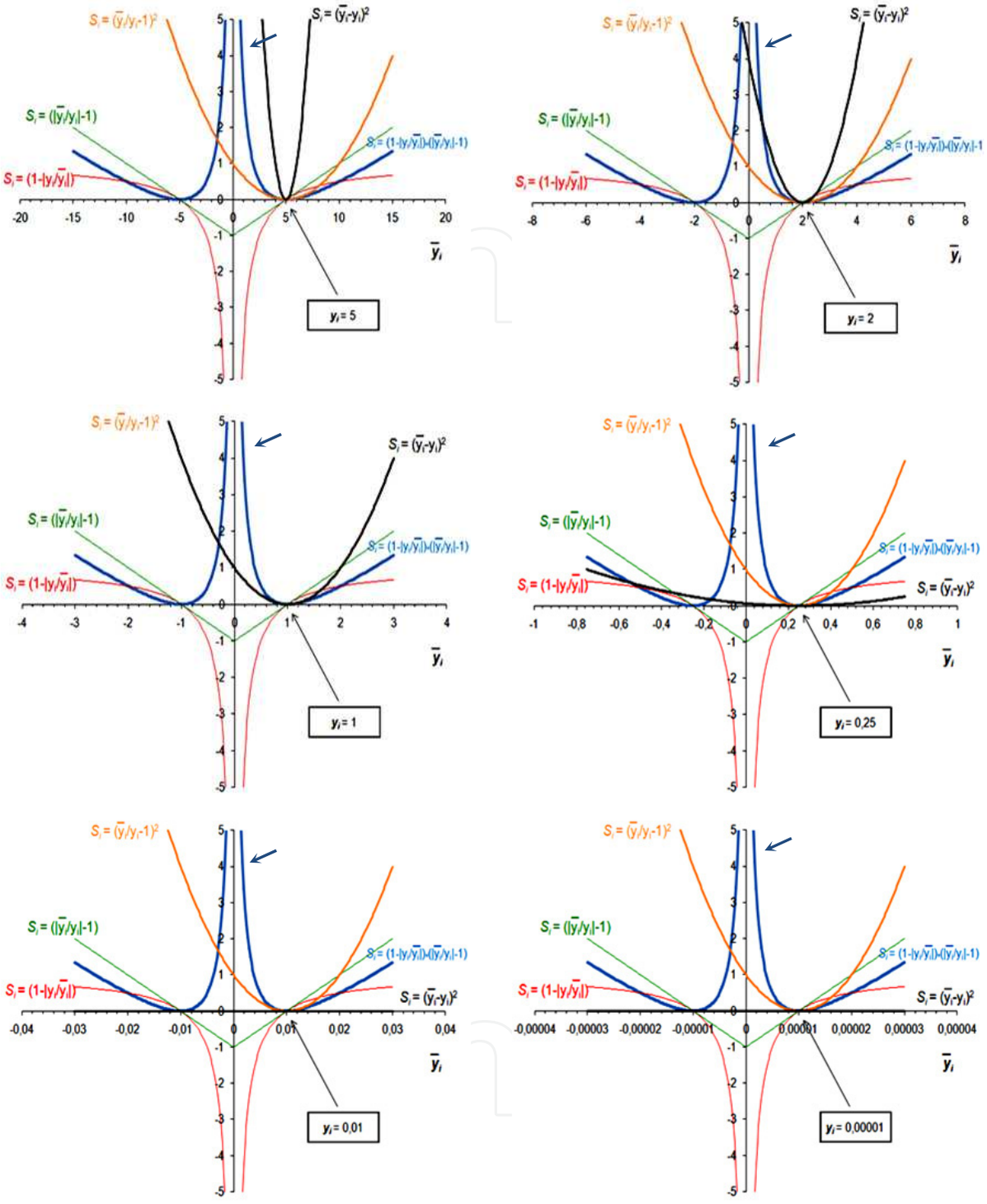


**Figure 13.** Approximation criterion functions for different approximated values $y_i$ for the $(-3y_i, 3y_i)$ interval – arrow for equation (32a)

All advantages and disadvantages of the above presented LSM approximation criteria can be seen on the graphs above, in particular:

- significant dependence of values of components of the sum $S$ (formula (15)) on the approximated value $y_i$;

- invariability of values of components of sums $S^*$ (formula (20)) and $S^{**}$ (formulae (32) and (32a)) on all the graphs, i.e. for any approximated value $y_i$;
- no response of the components of sums $S$ and $S^*$ to the $\bar{y}_i \rightarrow 0$ effect and dynamic change in the components of the sum $S^{**}$ near value $\bar{y}_i = 0$.

The only curve that changes in the graphs presented in Fig. 13 is the plot for components of the sum $S$ graph, i.e. for the standard form of the LSM.

Result of approximation with criterion (32a) applied is shown in Fig. 10b – for data sets with no extrapolation points. The same approximation for only 1 specimen tested at different $R$ is shown in Fig. 14a, and for only 2 specimens tested at different $R$ - in Fig. 14b.

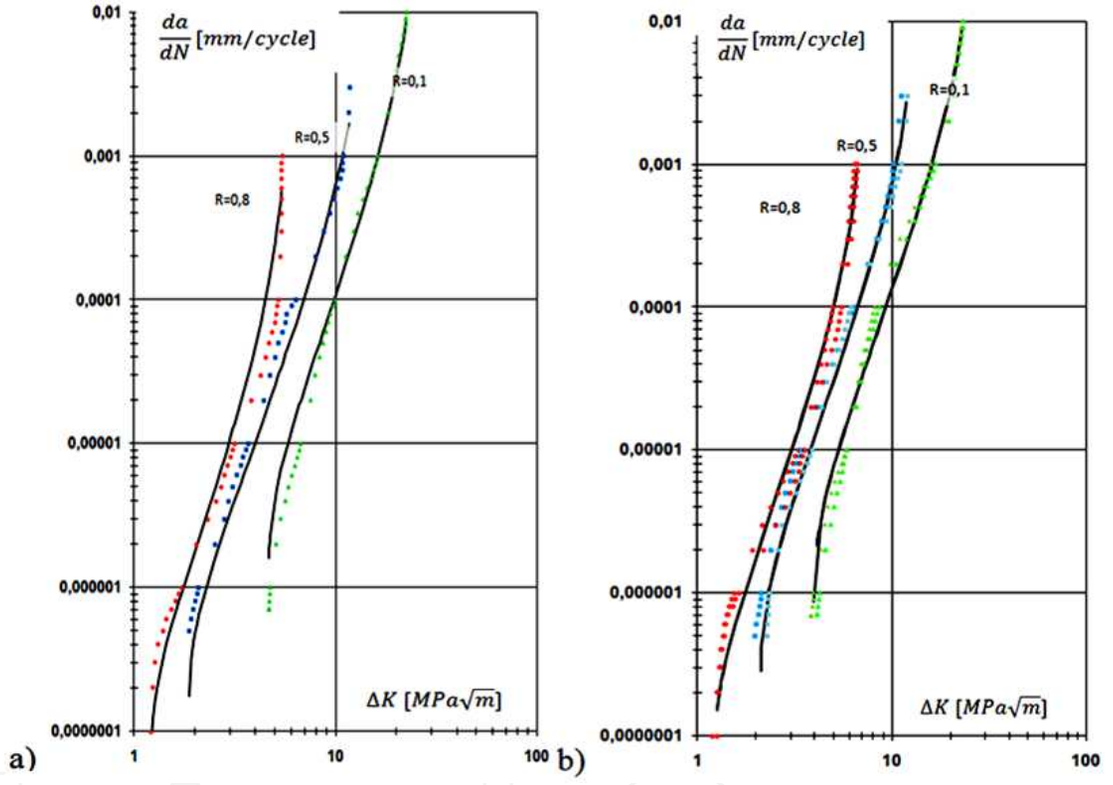


**Figure 14.** Approximation of *da/dN=f(ΔK)* data in different variants with the NASGRO equation, LSM modified according to formula (32a)

Exemplary results of approximation for different test data (with slightly smaller scatter between individual *da/dN-f(ΔK)* curves) is presented in Fig. 14.

Favorable effects of the approximation (in comparison with results showed in Fig. 1) after implementation of the modified LSM criterion can easily be seen. They tend to represent all the test data, within the whole range of data variability, independently of their absolute values, independently of the number of described curves – 3 (Fig. 14a), 6 (Fig. 14b), 9 (Fig. 10b). This effect has been achieved only by modifying the LSM criterion, since the idea underlying the approximation method for all the presented graphs is identical – the minimum of the sum of squared deviations between the approximated test data and the approximating values.

### 3.4. Regression of dependences in the NASGRO equation

Approximation of curves $da/dN$-$\Delta K$ substantially depends on preset values of parameters $K_c$ and $K_{th}$. Hence, it is very important whether they can be determined on the grounds of the test data only (if they cover the whole range of the curve, i.e. $10^{-7}$ through $10^{-2}$ mm/cycle, which is not always easy to reach), or whether they need any other method/way to be determined, e.g. formula (2), functional dependences of the type $\Delta K_{th} = f(R)$ and $K_c = f(R)$, or the above-mentioned extrapolation. The above-discussed results of extrapolation correspond to the case when both the parameters show constant values for all the approximated curves. The plots for the test data show, however, that they depend on the stress ratio $R$ – for each of nine experimentally gained curves parameters $\Delta K_{th,i}$ and $K_{c,i}$ can be estimated and the data gained can then be used to determine dependences $\Delta K_{th} = f(R)$ and $K_c = f(R)$, including coefficients for equation (2).

Formulae (2) and (2a) are special cases of a general formula of the following form:

$$\Delta K_{th} = \Delta K_0 \cdot \left( \frac{a}{a + a_0} \right)^{\frac{1}{2}} \left( \frac{(1-R)(1-A_0)}{(1-f)} \right)^{(C + C_{th} R)} . \tag{33}$$

Having re-arranged this formula, the following is arrived at:

$$\log(\Delta K_{th}) = \log\left( \Delta K_0 \cdot \left( \frac{a}{a + a_0} \right)^{\frac{1}{2}} \right) + C \log\left( \frac{(1-R)(1-A_0)}{(1-f)} \right) + C_{th} R \log\left( \frac{(1-R)(1-A_0)}{(1-f)} \right) \tag{34}$$

and then:

$$\begin{aligned} \log(\Delta K_{th}) - \tfrac{1}{2} \log\left( \frac{a}{a + a_0} \right) &= \log(\Delta K_0) + C \log\left( \frac{(1-R)(1-A_0)}{(1-f)} \right) + \\ &+ C_{th} R \log\left( \frac{(1-R)(1-A_0)}{(1-f)} \right) \end{aligned} \tag{35}$$

which can be described with the linear-regression equation as:

$$y = m_0 + m_1 F(R) + m_2 R F(R), \tag{36}$$

where $F(R) = \log\left( \frac{(1-R)(1-A_0)}{(1-f)} \right)$,

and the corrected value of the threshold range of the stress intensity factor is:

$$y = \log(\Delta K_{th}) - \tfrac{1}{2} \log\left( \frac{a}{a + a_0} \right).$$

Having found coefficients $m_0$, $m_1$, $m_2$ of the regression equation (36) we can calculate coefficients of equation (33):

$$C_{th} = m_2, \quad C = m_1 \quad \text{and} \quad \Delta K_0 = 10^{m_0} \tag{37}$$

at the same time, value of the $\Delta K_{th}$ function is calculated from the regression equation by formula:

$$\Delta K_{th} = 10^{y} \cdot \left( \frac{a}{a + a_0} \right)^{\frac{1}{2}}. \tag{38}$$

So, if we have data sets ($R_i$, $\Delta K_{th,i}$, $a_i$) – in the case under analysis there are 9 such sets – we automatically can find coefficients by formula (37), thus reducing the number of coefficients of the NASGRO equation to approximate the test data, which we are looking for.

Since there is no similar dependence for the $K_c$, parameter, the relationship $K_c = f(R)$ can be found in the same way (i.e. using the test data) from the ordinary linear regression $K_c = m_0 + m_1 R$ and also use it to describe 9 experimentally gained curves.

Functions $\Delta K_{th} = f(R)$ and $K_c = f(R)$ found in this way with the test data applied are shown in Fig. 15, whereas Fig. 16 illustrates effect of approximating curves $da/dN$-$\Delta K$ in the case given consideration.

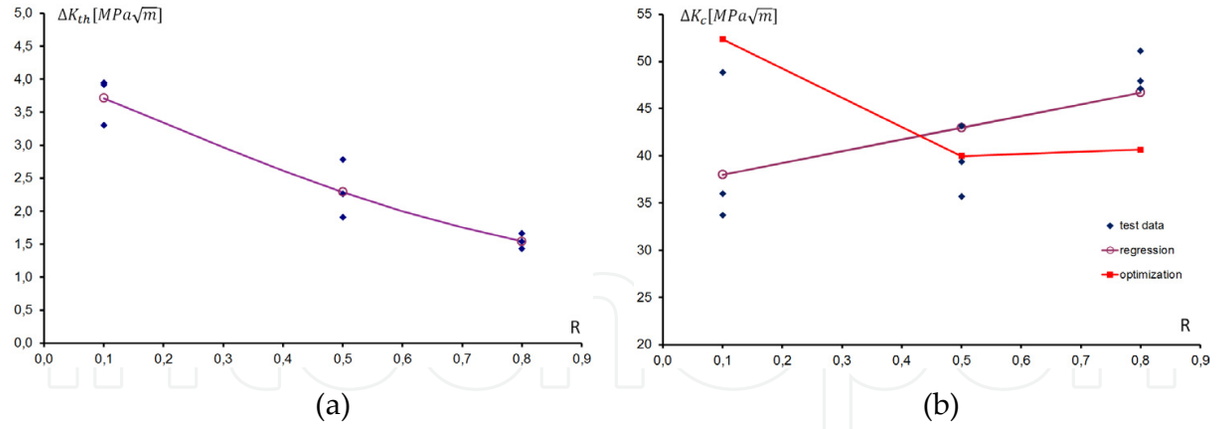


**Figure 15.** Functions a) $\Delta K_{th} = f(R)$ by formula (33) and b) $K_c = f(R)$ - regression

Evident is good fit of analytical description in both the critical and threshold ranges, whereas worse - in the middle section. The *ad hoc* accepted linear regression for the experimentally found relationship $K_c = f(R)$ not too precisely describes this relationship (straight line in Fig. 15, correlation coefficient reaches in this case the 0.3 level). Optimisation of values of the $K_c$ coefficient for $R = 0.1$; 0.5 and 0.8 (here denoted as $K_c$*) with the LSM method to reach the minimum deviation error (32) results in the $da/dN$-$\Delta K$ curves

approximating courses as in Fig. 16b. The curve illustrating the $K_c^* = f(R)$ dependence is in this case a broken line shown in Fig. 15b, which – easy to see – considerably strays away from the linear dependence. This proves that, among other things, one cannot *ad hoc* impose any form upon it. It can be assumed that for a larger number of experimentally gained curves, including the wider scope of values of $R$, the suggested method of determining the relationship $K_c = f(R)$ will offer better results that better correspond to the actual dependence and will remain useful for approximating the $da/dN$-$\Delta K$ curves. The broken-line curve, as that resulting from the optimisation process, may be described with, e.g. a straight line or a quadratic equation (as in Fig. 17) and used as a component of the theoretical (analytical) description of the test data with the NASGRO equation. In the case of a straight line, the correlation coefficient increases up to approx. 0.78 for the polynomial. Obviously, with three points $K_c^*$ the correlation is complete, but if the scope of values of the asymmetry coefficient was greater, i.e. there would be more experimentally gained curves of different values of $R$ (then the number of these points would increase), one should also expect high correlation for the relationship $K_c = f(R)$.

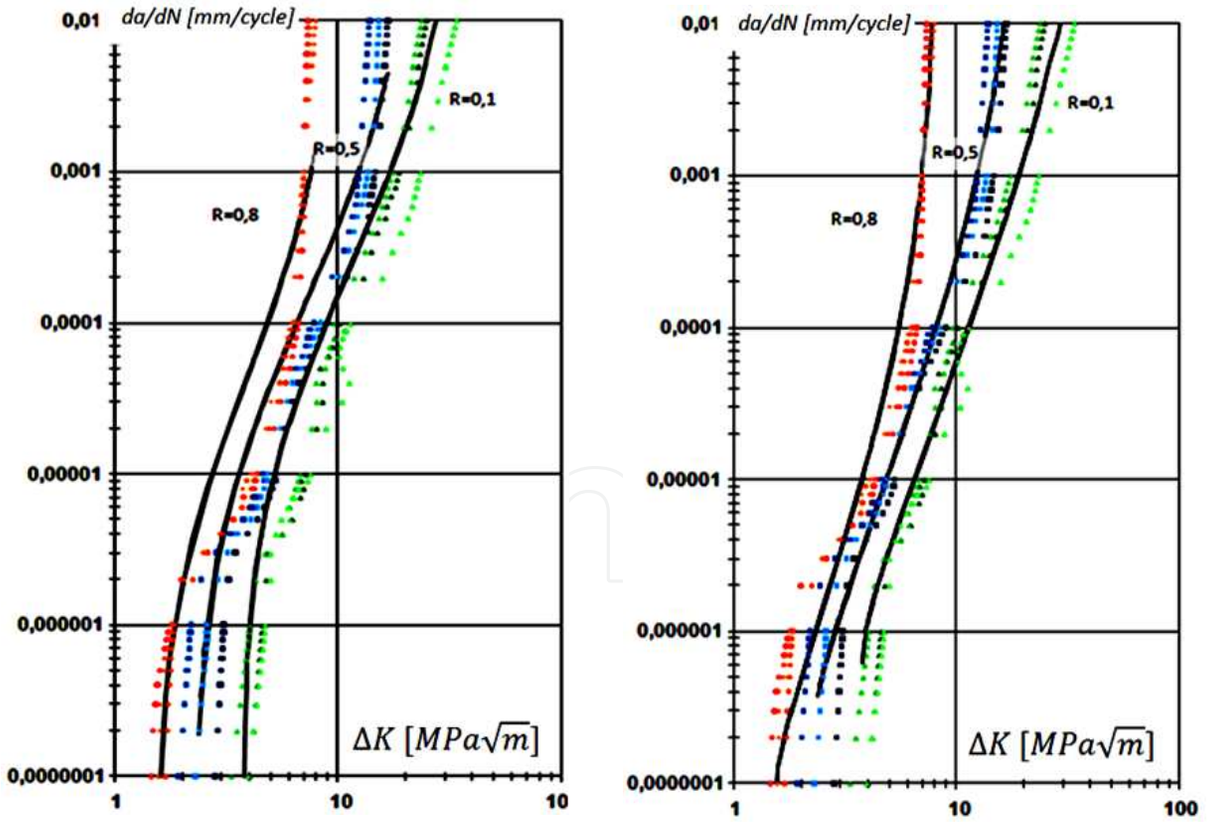


**Figure 16.** Approximation of curves $da/dN$-$\Delta K$ with the NASGRO equation, modified by formula (32) LSM, with extrapolated mapping points according to the MRCM: a) with regression applied as in Fig. 15, b) with optimisation for values of coefficients $K_c$*

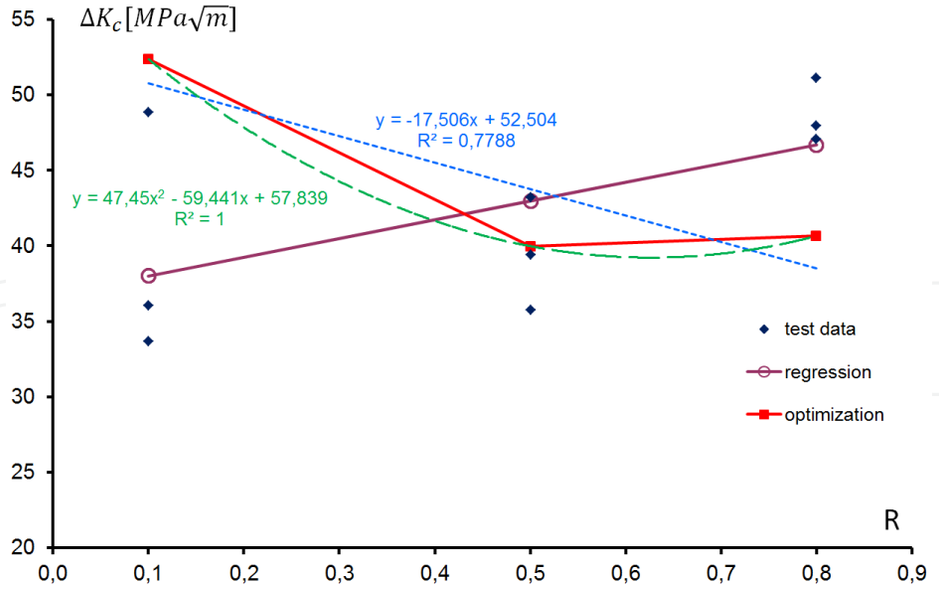


**Figure 17.** Linear $K_c = f(R)$ and polynomial $K_c^* = f(R)$ functions to optimise theoretical (analytical) description of curves $da/dN$-$\Delta K$

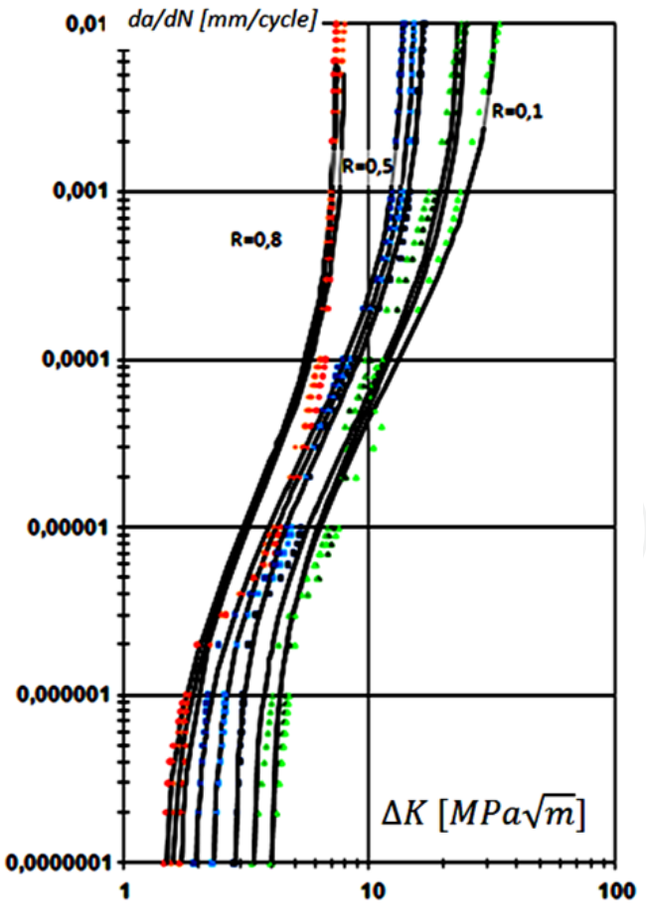


**Figure 18.** Curves $da/dN$-$\Delta K$ with coefficients $\Delta K_{th}$ and $K_c$ individually fitted to each experimentally gained curve

If we use values of $\Delta K_{th}$ i $K_c$ coefficients in forms determined not with the above-mentioned regression and optimisation methods, but as ones individually found for each of the experimentally gained curves ($\Delta K_{th,ind}$ i $K_{c,ind}$), the theoretical (analytical) description by means of the NASGRO equation - with the above-described methodology of finding other coefficients applied - should give even better result, see Fig. 18.

This variant of the theoretical (analytical) description is of only little practical importance, however, it shows that both the above-described methodology of analysis and the way of finding coefficients of the NASGRO equation result in correct description of experimentally found curves of fatigue-crack propagation and may be applied to this and similar categories of research issues.

## 4. Conclusion

Application of the Least Square Method in its classical form to determine coefficients of the NASGRO equation that describes fatigue crack propagation curve is ineffective, since data of the approximated function $da/dN=f(\Delta K)$ take values from the range of a few orders of magnitude, measuring points of the curves are irregular and in different numbers distributed in the graph (in threshold, stable-increase, and critical ranges), and subject to approximation are also several curves grouped in several sets (for different values of $R$).

The paper offers some techniques to modify the LSM criterion to significantly improve approximation results. These include:

- modification of the approximation-method criterion,
- smoothing of the experimentally gained curves to eliminate slight random disturbances resulting from, e.g. data recording process,
- different variants of calculating the derivative $da/dN$,
- regular mapping of the experimentally gained curves in the form of selected points,
- regression for points that represent (map) the experimentally gained curves to find coefficients of the crack growth equation,
- regression or optimisation of the description of partial dependences of the NASGRO equation as based on experimental data.

Values of parameters to be found as well as quantitative and qualitative results of performed approximations and theoretical (analytical) description are affected by, among other things, the number of tests that produce experimental data, and configurations thereof.

They provide a wider or narrower range of variability of parameters of significance that affect the courses of curves $da/dN$-$\Delta K$, and also enable determination of accuracy and repeatability of obtained results. Reliability of the theoretical (analytical) description increases and the description itself better characterises properties of the material under examination if there are tens of curves gained experimentally from tests conducted for many (e.g. 5, 7, or 9) levels of the stress ratio $R$ , for a wider range thereof, e.g. 0.2 through 0.9.

The proposed modification of the LSM criterion offers better fit of results of the test data approximation (unachievable with the classical LSM method). These effects are as follows:

- the provision of equal "weights" of each of the test data points in the total sum that determines this criterion (i.e. the sum of differences between approximated and approximating values) – independently of the magnitude of difference between values of data subject to approximation and that of difference between the approximated and approximating values,
- high effectiveness while approximating single, several, as well as a great number of sets/curves of test data,
- it becomes even more precise as the test data from the same (research-testing) groups show smaller scatter,
- may be used in other analyses of the same type related with test data regression, since it offers an all-purpose approach not related to propagation curves $da/dN$-$\Delta K$.

## Author details

Sylwester Kłysz
*Air Force Institute of Technology, Warsaw, Poland*
*University of Warmia and Mazury in Olsztyn, Poland*

Andrzej Leski
*Air Force Institute of Technology, Warsaw, Poland*

## 5. References

AFGROW Users Guide And Technical Manual. (2002). *AFRL-VA-WP-TR-2002-XXXX,* Version 4.0005.12.10, James A. Harter, Air Vehicles Directorate, Air Force Research Laboratory, WPAFB OH 45433-7542

ASTM E647 Standard test method for measurement of fatigue crack growth rates

Bukowski, L. & Kłysz, S. (2003). Compliance curve for single-edge notch specimen. *Zagadnienia Eksploatacji Maszyn*, No. 2(134), pp. 95-104

Elber, W. (1970). Fatigue crack closure under cyclic tension, *Eng. Fracture Mechs.*, Vol.2, pp. 37-45

Forman, R.G.; Kearney, V.E. & Engle, R.M. (1967). Numerical analysis of crack propagation in cyclic loaded structures, *J. Bas. Engng,* Vol.89, pp. 459-464

Forman, R.G.; Shivakumar, V.; Cardinal, J.W.; Williams, L.C. & McKeighan, P.C. (2005). Fatigue crack growth database for damage tolerance analysis, *DOT/FAA/AR-05/15,* U.S. Dep. of Transportation, FAA Office of Aviation Research, Washington, DC 20591

Fuchs, H.O. & Stephens, R.I. (1980). Metal fatigue in engineering, A Willey-Interscience Publication

Huang, X.P.; Cui, W.C. & Leng, J.X. (2005). A model of fatigue crack growth under various load spectra, *Proc. of 7th Int. Conf. of MESO*, Montreal, Canada, pp. 303–308

Kłysz, S. (2001). Fatigue crack growth in aircraft materials and constructional steel with overload consideration, (in Polish), *Air Force Institute of Technology Publication*, ISSN 1234-3544, Warsaw, Poland

Kłysz, S. & Lisiecki, J. (2009). Report of fatigue crack growth rate testing, (in Polish), *Laboratory for Material Strength Testing Report,* No. 1d/09, Air Force Institute of Technology, Warsaw, Poland

Kłysz, S.; Lisiecki, J. & Bąkowski, T. (2010a). Modification of the east-squares method for description of fatigue crack propagation, *Research Works of Air Force Institute of Technology*, ISSN 1234-3544, No.27, pp. 85-91, Warsaw, Poland

Kłysz, S.; Lisiecki, J. & Klimaszewski, S. (2010b). Analysis of crack propagation curve description for ORLIK aircraft fuselage skin material, (in Polish), *Technical News*, No 1(31), 2(32), pp.148-151, Lvov, Ukraine

Kłysz, S.; Lisiecki, J.; Leski, A. & Bąkowski, T. (2012). Least squares method modification applied to the NASGRO equation, *J. of Applied and Theoretical Mechanics*, Warsaw, Poland (in printing)

Kłysz, S.; Lisiecki, J.; Leski, A. & Bąkowski, T. (2012). Modification of the LSM criteria to approximate test data for fatigue crack growth rate, *J. of Applied and Theoretical Mechanics*, Warsaw, Poland (in printing)

Lisiecki, J. & Kłysz, S. (2007). Report of fatigue crack growth rate testing, (in Polish), *Laboratory for Material Strength Testing Report,* No. 8c/07, Air Force Institute of Technology, Warsaw, Poland

Murakami, Y. (Ed.). (1987). Stress Intensity Factors Handbook, *The Society of Materials Science,* Pergamon Press, Japan

NASGRO® Fracture Mechanics and Fatigue Crack Growth Analysis Software. (2006). v5.0, NASA-JSC and Southwest Research Institute

Newman, J.C. jr. (1992). Fastran II – A fatigue crack growth structures analysis program, *NASA TN 104159,* Langley Res. Centre, Hampton, VA

Paris, P.C. & Erdogan, A. (1963). A critical analysis of crack propagation laws, *J. Bas. Engng*, No.85, pp. 528-534

Skorupa, M. (1996). Empirical trends and prediction models for fatigue crack growth under variable amplitude loading, *ECN-R-96-007,* Netherlands Energy Research Foundation

Smith, R.A. (Ed.). (1986). *Fatigue Crack Growth. 30 Years of Progress,* Pergamon Press, Cambridge, UK

Taheri, F.; Trask, D. & Pegg, N. (2003). Experimental and analytical investigation of fatigue characteristics of 350WT steel under constant and variable amplitude loadings, *J. of Marine Structure*, No.16, pp. 69-91

Wheeler, O.E. (1972). Spectrum loading and crack growth, *Trans. ASME, J. Basic Eng.,* 94, 181

White, P.; Molent, L. & Barter, S. (2005). Interpreting fatigue test results using a probabilistic fracture approach, *Int. J. of Fatigue*, No.27, pp. 752-767

Willenborg, J.; Engle, R.M. & Wood, H.A. (1971). A crack growth retardation model using an effective stress concept, AFFDL-TR-71-1

Zhao, T. & Jiang Y. (2008). Fatigue of 7075-T651 aluminum alloy, *Int. J. of Fatigue*, No.30, pp. 834-849



IntechOpen